Vehicle Dispatching and Routing of On-Demand Intercity Ride-Pooling Services: A Multi-Agent Hierarchical Reinforcement Learning Approach

Jinhua Si^a Fang He^{a*} Xi Lin^{a,b} Xindi Tang^c

^aDepartment of Industrial Engineering, Tsinghua University, Beijing 100084, P.R. China

^bDepartment of Civil Engineering, Tsinghua University, Beijing 100084, P.R. China

^cSchool of Management Science and Engineering, Central University of Finance and Economics, Beijing 100081, P.R. China

July 14, 2023

Abstract

The integrated development of city clusters has given rise to an increasing demand for intercity travel. Intercity ride-pooling service exhibits considerable potential in upgrading traditional intercity bus services by implementing demand-responsive enhancements. Nevertheless, its online operations suffer the inherent complexities due to the coupling of vehicle resource allocation among cities and pooled-ride vehicle routing. To tackle these challenges, this study proposes a two-level framework designed to facilitate online fleet management. Specifically, a novel multi-agent feudal reinforcement learning model is proposed at the upper level of the framework to cooperatively assign idle vehicles to different intercity lines, while the lower level updates the routes of vehicles using an adaptive large neighborhood search heuristic. Numerical studies based on the realistic dataset of Xiamen and its surrounding cities in China show that the proposed framework effectively mitigates the supply and demand imbalances, and achieves significant improvement in both the average daily system profit and order fulfillment ratio.

Keywords: Intercity; Ride-pooling; Vehicle Dispatching; Multi-agent Hierarchical Reinforcement Learning

1 Introduction

Conventional intercity bus services are facing increasing operational pressures. The number of intercity bus users in many countries has declined significantly in recent years (Ganji et al., 2021). The scale of the intercity bus industry in China, where more than 70% passenger trips are delivered by road transport, has been shrinking over the past decade. A large number of bus stations

^{*}Corresponding author. E-mail address: fanghe@tsinghua.edu.cn.

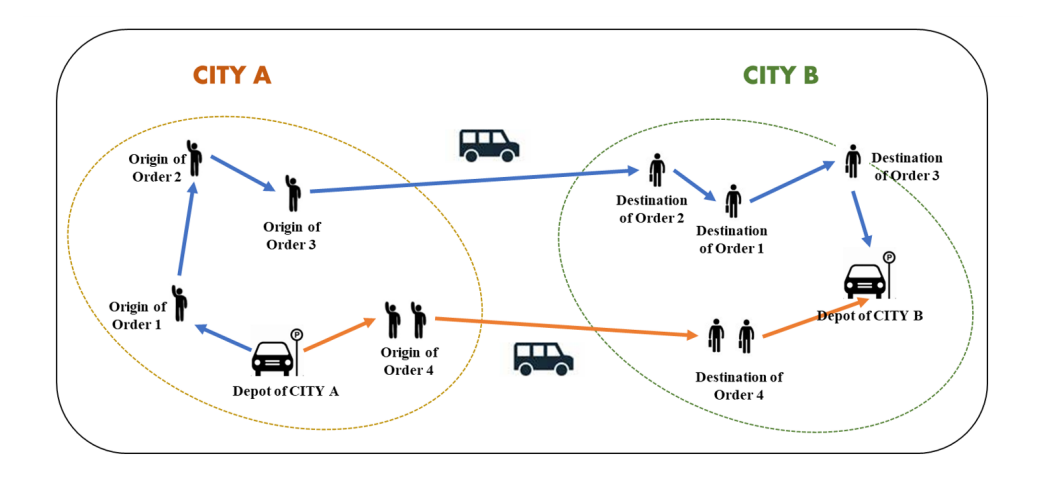


Figure 1: Intercity passenger transport in a pooled-ride manner.

in China shut down due to continued losses, and the nationwide number of passenger vehicles has decreased by 30.06% compared to 2015 (MOT, 2022). The intercity bus industry in the United States also began shrinking after 2015. Greyhound, which operates the largest intercity bus service in North America, reduced its operations by 16% between 2016 and 2020 (Schwieterman et al., 2021). The possible reasons include two folds. From the *supply* perspective, the steady increase in car ownership compresses the demand for short-haul bus lines, while the infrastructure construction of high-speed railways and airlines tends to be improved in more regions, delivering fatal blows to many longer-haul bus lines. From the *demand* perspective, people's travel behaviors are reshaped in the mobile Internet era, paying more attention to convenience, comfort, and privacy when traveling. Conventional intercity buses' attractiveness is weakened by the heightened competition from other transport modes.

With the development of mobile Internet and the proliferation of smartphones, the intercity ride-pooling service within city clusters is becoming a promising direction for the digital transition and demand-responsive upgrading of the conventional intercity bus service. As an emerging travel mode, it utilizes smaller capacity vehicles to carry fewer passengers in one trip, providing door-to-door service for each passenger. Similar to urban ride-hailing platforms, a computing center makes centralized decisions in real time based on the information of requests and available vehicles. Each order is expected to specify the number of passengers, the locations for pick-up and drop-off in different cities, the time windows, and other necessary information. The computing center assigns orders to vehicles precisely and plans the flexible routes for each vehicle to pick up passengers in the departure city and deliver them to the destination in a pooled-ride manner, as shown in Figure 1.

The advantages of intercity ride-pooling services in city clusters are mainly manifested in three aspects. The *first* advantage is replacing the traditional fixed-schedule service with a flexible ride-hailing service. The demand-responsive transit system, which has demonstrated its remarkable effectiveness in significantly enhancing the travel experience within urban public transport over the last decade (Wang and Yang, 2019; Liu and Ouyang, 2021; Vansteenwegen et al., 2022), holds great promise for delivering a more convenient and diversified travel experience in intercity transport. The demand-responsive services can also enhance system efficiency by matching supply and demand more intelligently and efficiently. The *second* advantage lies in the ability to

plan fully flexible routes for each vehicle instead of fixed routes, offering door-to-door services to passengers. With the gradual expansion of urban areas and increased traffic congestion, the generalized cost for passengers concentrating at bus stations in the city has increased dramatically, which makes door-to-door services increasingly appealing and advantageous. The *third* advantage is focusing on providing services for the intercity demand within a city cluster. The highly developed city cluster has become an increasingly significant geographic unit under the rapid urbanization process, where the strong socioeconomic connections between the cores and the peripheries brew up strong intercity travel demand (Fang and Yu, 2017). Road passenger transport is still competitive within city clusters, especially for those clusters with relatively low railway coverage. Rather than being subordinated to a fixed line between two cities, vehicles can be dispatched to any city within the cluster according to demand fluctuation, which can resolve the spatial imbalance between supply and demand.

While the aforementioned advantages highlight a promising market for intercity ridepooling services within city clusters, there are still several issues that hinder the development of this innovative service. The core is how to build a highly effective and intelligent fleet operations strategy for the sophisticated dynamic system and unique scenarios of intercity travel. From the perspective of macroscopic spatiotemporal allocation of vehicle resources, platforms need to implement dynamic dispatching of fleets among multiple cities to reduce the gap between available seats and potential demand between each city pair in future periods. Extensive explorations have been conducted in the operational strategy optimization in related fields, such as urban ride-hailing and ride-sourcing platforms(Xu et al., 2018a; Tang et al., 2020; Guo et al., 2021; Kullman et al., 2022). From the perspective of microscopic order-matching and vehicle routing, the platform needs to solve the multi-vehicle pooled-ride routing problem to maximize the profit of each route in an online manner, which is a variant of the Pickup and Delivery Problem with Time Windows (PDPTW) or Dial-a-Ride Problem (DARP) that has been investigated for over 40 years (Cordeau, 2006; Ropke and Pisinger, 2006). The fleet operations strategy is based on the integrated optimization of macroscopic fleet dispatching and microscopic pooled-ride vehicle routing, which has been barely touched on in existing literature under intercity scenarios. The coupling structure of vehicle resource allocation among cities and pooled-ride routing for each vehicle makes it difficult to devise an efficient fleet management strategy at the city cluster level using model-based approaches. Additionally, the differences between intracity and intercity travel lead to different optimization frameworks for ride-pooling services. The intercity demand-responsive transport system faces greater challenges in coping with demand peaks due to longer travel times. Consequently, intercity ride-pooling services must make dispatching decisions based on supply and demand dynamics in a longer-term perspective. Furthermore, relocation of idle vehicles, which is an effective way to achieve future spatial balance, is generally unreasonable in intercity ride-pooling services due to high travel costs. The intercity travel demand within a city cluster can be clustered into several mutually independent intercity lines, and the platforms have to allocate vehicle resources to lines across broader temporal and spatial dimensions.

This study proposes an online two-level framework that effectively and dynamically aggregates ride-pooling orders in city clusters, dispatches fleets among regions to alleviate intercity supply and demand imbalances, and makes decisions on vehicle routing within origin and destination cities. The *dispatching level* (upper level) assigns idle vehicles to intercity lines based on global demand and supply information. The dispatching decisions for each city are derived synergistically using a novel multi-agent hierarchical reinforcement learning method, named multi-agent feudal networks (MFuN), to enhance agent cooperation and far-sighted assignment.

The *routing level* (lower level) uses adaptive large neighborhood search methods (ALNS) to solve the order-vehicle matching and pooled-ride routing problems at each time interval based on the decisions of the dispatching level. The two-level framework can provide online operational decisions while avoiding myopic actions with the guidance of deep reinforcement learning. The system aims to improve both the system profit and order fulfillment ratio, enabling service to more passengers within their reserved time windows. The main contributions of this study can be summarized as follows.

- This study focuses on the online fleet operations of on-demand intercity ride-pooling services, while the applications of demand-responsive services in the realm of intercity transport have received scarce research attention thus far. The coupling of vehicle resource allocation among cities and multi-vehicle pooled-ride routing problems brings challenges for proposing an integrated model for dispatching and routing. We also take into account the distinctive attributes of intercity travel when developing strategies, including long travel times and high intercity costs.
- We propose an integrated online operational framework for intercity ride-pooling services within a city cluster. The framework comprises two levels, with the upper level dedicated to addressing vehicle resource allocation among cities in the long term, and the lower level focusing on dynamic routing. At each dispatching horizon, the upper level of the framework optimizes the distribution of vehicle resources within a city cluster by dispatching vehicles to intercity lines to mitigate the spatiotemporal imbalances between supply and demand. At each matching interval with a shorter time scale, the lower level solves dynamic DARP for each intercity line respectively to enable efficient online management of the fleet at the scale of city clusters.
- We take advantage of a novel multi-agent hierarchical reinforcement learning method, named MFuN, in the upper level of the framework, to develop a non-myopic strategy for the stochastic dynamic vehicle resource allocation problem. MFuN shows favorable performance in promoting agent cooperation and capturing transition patterns in system states over extended horizons, and ensures that the actions of each agent contribute to maximizing the long-term profits of the entire system.
- We acquire realistic operational data of intercity ride-pooling services to evaluate the effectiveness of our framework. The numerical experiments conducted reveal that the proposed framework can develop proactive operational strategies to alleviate the spatiotemporal imbalance between supply and demand, leading to remarkable performance enhancements on both system profit and order fufillment ratio.

The remainder of this paper proceeds as follows. Section 2 reviews recent literature addressing DARP and fleet dispatching problems. Section 3 specifically portrays the modeling of the problem. Section 4 introduces the proposed two-level operational framework. Section 5 conducts numerical experiments on two toy networks and one realistic network to demonstrate the optimization effectiveness under various supply and demand scenarios, and provide managerial insights for the platform operations. Finally, we summarize the study and provide an outlook on future research in section 6.

2 Literature Review

As an emerging service mode motivated by customized travel preferences and the growing volume of intercity population movements, the online operations of intercity ride-pooling service in city cluster has not been well investigated in the literature. Nevertheless, researchers have made several progress in solving related problems, such as the pooled-ride routing problem and urban demand-responsive fleet dispatching problem.

Multi-vehicle pooled-ride routing problem is a variant of the Pickup and Delivery Problem with Time Windows (PDPTW) or Dial-a-Ride Problem (DARP) (Ho et al., 2018). This problem can be formulated as a mixed-integer linear program (MILP) problem, and existing solution methods can be categorized into heuristic methods (Ropke and Pisinger, 2006; Naccache et al., 2018; Goeke, 2019; Guo et al., 2022) and exact methods(Cordeau, 2006; Gschwind and Irnich, 2015; Braekers and Kovacs, 2016; Luo et al., 2019). However, for large-scale problems, exact algorithms such as branch-and-cut algorithms and branch-and-price algorithms are usually unable to provide optimal or even feasible solutions within an acceptable time, so heuristic algorithms such as neighborhood search algorithms are more widely used in realistic problems. Adaptive large neighborhood search (ALNS), first proposed by Ropke and Pisinger (2006), is one of the most effective heuristic algorithms to solve realistic multi-vehicle dial-a-ride problems with pick-up and delivery time windows. ALNS utilizes multiple removal and insertion operators to enhance the movement in solution space in a simulated annealing metaheuristic manner. Subsequent research has proposed many detailed techniques to improve the performance of the algorithm or to solve the variants of DARP (Demir et al., 2012; Ghilas et al., 2016; Gschwind and Drexl, 2019; Sun et al., 2020a).

The aforementioned routing algorithms for DARP are widely used in urban demandresponsive services such as flexible bus systems and ride-sharing services. Studies on the operations of these systems not only consider vehicle routing but also fleet scheduling and dispatching, which are similar to our study to some extent. Flexible bus systems in practice can be classified into two categories. The first category is semi-flexible that each bus travels along a standard route and can deviate from the predetermined route to serve emerging demand, while the second category is fully flexible that routes and timetables are totally determined based on demand (Vansteenwegen et al., 2022). Some studies model the semi-flexible bus scheduling and routing as static problems, among which the majority combine candidate stops into routes based on demand spatial distribution (Czioska et al., 2019; Sun et al., 2020b), while others collaboratively optimize the selection of bus stops and suggestions for pick-up locations (Melis and Sörensen, 2022b). Matching of new orders and dynamic adjustment of routes are considered to develop dynamic models in some literature (Fielbaum et al., 2021; Tafreshian et al., 2021; Melis and Sörensen, 2022a). In the literature of fully flexible bus systems, the online vehicle routing problems are usually modeled as deterministic dynamic DARP and solved by the methods mentioned above(Agatz et al., 2012; Braekers and Kovacs, 2016; Huang et al., 2020; Guo et al., 2022; Wu et al., 2022). Some literature uses stochastic optimization to capture the uncertainty of demand distribution and detour time (Lee et al., 2021).

Besides the vehicle routing problems in the context of ride-pooling, we also review the studies on the fleet operations strategies for urban ride-hailing services, which are one of the most extensively investigated and applied domains of demand-responsive transport. In urban ride-hailing services, vehicles typically fulfill only one order during a single trip. Therefore, the operational strategy of the fleet in urban ride-hailing services is primarily based on the vehicle-

order matching problem rather than the vehicle routing problem. The greedy algorithms have been widely applied in practice but have been proven to be inefficient by Maciejewski et al. (2016). The batch matching optimization can be formulated as a bipartite matching problem (Tong et al., 2016; Qin et al., 2021b). Some literature proposes a dynamic optimization model to determine the optimal matching interval and radius (Guo et al., 2020; Yang et al., 2020; Qin et al., 2021a). Reinforcement learning methods for dynamic matching also have gained immense attention in recent years to prevent short-sighted decisions (Xu et al., 2018a; Tang et al., 2019; Qin et al., 2020).

Based on the aforementioned matching optimization of urban ride-hailing services, the spatiotemporal imbalance between supply and demand can be further mitigated by proactive vehicle dispatching methods. By leveraging extensive operational data, the platform can develop a sophisticated supply and demand prediction model, offering guidance for real-time vehicle dispatching (Ke et al., 2017; Guo and Zhang, 2020), which dispatch idle vehicles to regions with large demand gaps in advance. Methods for fleet dispatching problem in urban ride-hailing services can be broadly classified into two categories. The *first* category models the problem as a Markov decision problem and constructs various optimization models(Xu et al., 2018a). Yu and Shen (2019) study the urban ride-pooling services and designed an approximate dynamic programming algorithm to approximate its value functions. Lei et al. (2020) propose a two-layer framework, where the upper layer focuses on dynamic pricing and relocation, while the lower layer determines the passengers' choice behavior based on market equilibrium. Guo et al. (2021) employ a rolling-horizon robust optimization approach based on model predictive control (MPC) for vehicle location optimization.

The second category adopts model-free approaches to tackle large-scale fleet operations for ride-hailing services. Many studies use single-agent reinforcement learning to provide centralized decisions. Tang et al. (2020) designed a two-layer single-agent reinforcement learning framework to solve the problem of online dispatching, charging arrangement, and order matching for urban electric vehicles. Liu et al. (2022) propose a single-agent deep reinforcement learning approach for the vehicle dispatching problem, in which a single-agent queue is designed for dispatching multiple vehicles based on a global pruned action space. More studies utilize multiagent reinforcement learning (MARL) framework to derive dispatching and scheduling strategies based on the well-trained value functions (Xu et al., 2018a; Jin et al., 2019; Guo and Xu, 2020; Jiao et al., 2021; Kullman et al., 2022). In these studies, an agent is usually defined as a vehicle or vehicles within a grid, with eligible actions including repositioning to a certain area and fulfilling certain orders. The innovations of these studies are mainly focused on the application of frontier reinforcement learning techniques to enhance the model's effectiveness, such as the use of attention mechanisms and graph neural networks. Compared to single-agent reinforcement learning methods, multi-agent frameworks attain more efficient performance in large-scale problems, but their policies are decentralized that may sacrifice system-level optimality (Mao et al., 2020).

To summarize, although demand-responsive fleet management has garnered sustained attention in recent years, the distinctive characteristics of intercity ride-pooling services still pose challenges for the direct application of existing frameworks. Specifically, for the routing problem of each ride-pooling vehicle, the existing literature has proposed comprehensive methods for effective computation. However, applying routing algorithms at the city cluster level can result in a vast search space, while introducing intercity lines is able to simplify the multi-vehicle pooled-ride routing problem at the city cluster level into separate vehicle routing within each line. For the fleet dispatching, the aforementioned dispatching strategies for urban flexible bus systems and ride-hailing services are not directly applicable to fleet operations within a network comprising multiple cities. Intercity transport is based on a topology of city networks with relatively

long duration for intercity trips, and relocation of idle vehicles is generally not cost-effective. The most formidable challenge resides in the coupling between long-term vehicle resource allocation and dynamic vehicle routing, which has received scant attention in existing research. Both intercity dispatching and dynamic pooling are difficult to solve using model-based approaches, while realistic fleet operations necessitate an efficient online framework to integrate the optimization of these two levels.

3 Modeling

3.1 Problem settings

In our study, we consider fleet operations in the context of intercity ride-pooling services within a city cluster. The cluster $\mathcal{U} = \{1,...,n\}$ contains several interconnected cities, and the platform manages a fleet to fulfill intercity travel demands within the cluster in a pooled-ride manner. The demands with the same origin cities and the same destination cities can be clustered. Only orders in the same cluster can be pooled, which means that the orders served by a vehicle in one ride must originate from the same city and travel to the same city. It is assumed in this study that orders with different origin cities or different destination cities can not be simultaneously served by the same vehicle because visiting other cities en route will significantly increase the detour time for passengers on board. Under this assumption, the ride-pooling services within the city cluster can be split into services for a set of intercity lines $\mathcal{L} \subset \mathcal{U} \times \mathcal{U}$, in which each line $\ell \in \mathcal{L}$ starts from city $o^{\ell} \in \mathcal{U}$ and ends at city $d^{\ell} \in \mathcal{U}$ without visiting any intermediate city. Notice that ride-pooling service is not available for all pairs of cities within the cluster. The platform exclusively offers intercity lines between cities with sufficient demand for intercity travel, whereas the demand level between other city pairs can be so minimal that ride-pooling services cease to benefit from economies of scale. Furthermore, the lines in this study are different from the fixed lines of conventional intercity bus services. Conventional intercity buses travel along fixed routes on a fixed schedule, while vehicles in this study travel along fully flexible routes on each line. Instead of adhering to specific lines, each vehicle can be dynamically assigned to any line originating from its current city for upcoming rides.

From the *supply* perspective, the fleet dispatching is based on the directed graph $G(\mathcal{U}, \mathcal{L})$. We assume all vehicles in the fleet \mathcal{K} are identical in capacity and speed, they will clock in from different cities at different times to work continuously for no more than a preset time limit \bar{W} . The platform assigns orders to vehicles so that vehicles can pick up and deliver passengers in the planned sequence to complete a trip. Since intercity trips are relatively costly, relocation between cities is discouraged, and hence the platform only assigns idle vehicles to lines originating from the cities they are located. Furthermore, for the sake of long-distance transportation safety, drivers have to take a certain period of rest at the depot after finishing an intercity ride.

From the *demand* perspective, this study primarily focuses on providing services to ondemand orders, which require prompt service within a relatively short period after reservation (e.g., within 2 hours). Although intercity travel demands often exhibit long-term periodicity, the system faces challenges in handling abrupt fluctuations in demand caused by these on-demand orders. Each order includes information such as the number of passengers, origin, destination, time window, and selected line. Passengers are assumed to wait at the designated origins within the reserved time windows for pick-up, and the order will be forfeited if no matching vehicle arrives at the origin node within the specified time window. Passengers may also have require-

ments for the latest arrival time at their destinations, necessitating the platform to ensure that each passenger arrives before their respective reserved arrival time when planning vehicle routes.

3.2 Modeling framework

In this subsection, we briefly introduce the overall decision-making framework in fleet dispatching and vehicle routing of the intercity ride-pooling services. We discretize the daily time domain into T dispatching horizons of equal duration and the set of all horizons is denoted as T. Orders of each line ℓ emerge following a specific stochastic process throughout the day, which are added into the matching pool of each line respectively in real-time. The fleet operations within each dispatching horizon $t \in T = \{0, 1, ..., T-1\}$ contain two levels: *first*, the platform assigns idle vehicles to different lines or reserves them at their current cities; *second*, the platform plans a route for each vehicle to fulfill orders in the matching pool for each line respectively, which is illustrated in Figure 2 (a).

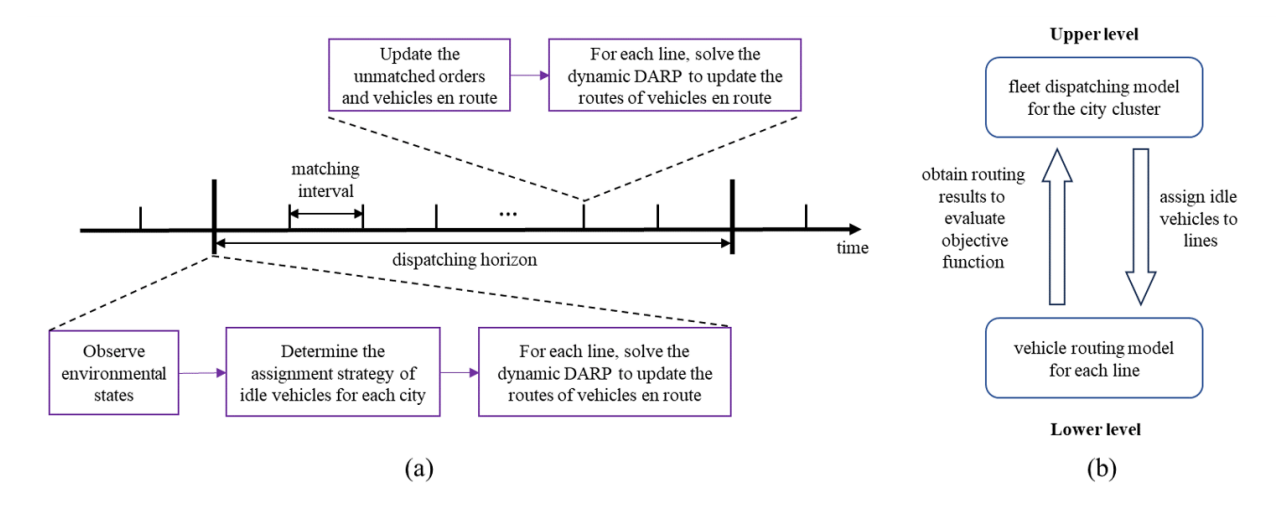


Figure 2: (a) Illustration of the dispatching horizons and matching intervals. (b) Interaction between two levels.

At the beginning of a dispatching horizon, the platform develops dispatching decisions for the current horizon based on the global supply and demand information, which determines the set of idle vehicles newly assigned to each line and the set of idle vehicles reserved in each city. A relatively short horizon may lead to no idle vehicles for assignment, while an excessively long horizon could compromise the effectiveness of the dispatching. Based on realistic operational data and numerical tests, we set the horizon duration as 20 minutes in this study. Each dispatching horizon is comprised of several matching intervals with equal lengths because the matching of unserved passengers should be achieved quickly to avoid order loss. In each matching interval, the planned routes of all vehicles en route are updated to match the orders in the matching pool. As a result, a horizon is composed of a set of batch-matching processes. The first batch matching is executed instantly after the assignment of idle vehicles, which can provide initial routes for vacant vehicles to fulfill orders, and the other batch matching in a horizon is executed at the beginning of each interval to update routing. The matching interval can be within the range of 0.5 to 2 minutes in practice. Based on this operational framework, the intercity fleet operations problem can be regarded as a two-level embedded fleet dispatching and vehicle routing problem.

The vehicle routing problem at the lower level is based on the decision of assigning vehicles to lines derived from the upper level, and the objective function of the fleet dispatching problem at the upper level is obtained by the routing results of the lower-level problem, as illustrated in Figure 2 (b).

3.3 The fleet dispatching model

The fleet dispatching problem at the upper level of the modeling framework can be described as a stochastic dynamic resource allocation problem (SDRAP) (Godfrey and Powell, 2002). Let $\hat{\mathcal{K}}_u^t$ denote the set of vehicles that enter the system to start working at the beginning of horizon $t \in \mathcal{T}$ at city $u \in \mathcal{U}$, $\tilde{\mathcal{K}}_u^t$ denote the set of vehicles that exit the system due to reaching limited work duration at the beginning of horizon t at city u, $\tilde{\mathcal{K}}_u^t$ denote the set of arrived vehicles at horizon t at city u, $\tilde{\mathcal{K}}_u^t$ denote the set of reserved vehicles at horizon t at city u. Then all available vehicle resources for assignment at horizon t at city t is t is t in t

$$\hat{\mathcal{K}}_{u}^{t} = \left(\bigcup_{v:(u,v)\in\mathcal{L}} \mathcal{N}_{uv}^{t}\right) \cup \bar{\mathcal{K}}_{u}^{t} \qquad \qquad t = 0, \forall i \in \mathcal{U}$$
 (1)

$$\hat{\mathcal{K}}_{u}^{t} \cup \check{\mathcal{K}}_{u}^{t} \cup \bar{\mathcal{K}}_{u}^{t-1} \setminus \tilde{\mathcal{K}}_{u}^{t} = \left(\bigcup_{v:(u,v)\in\mathcal{L}} \mathcal{N}_{uv}^{t}\right) \cup \bar{\mathcal{K}}_{u}^{t} \qquad \forall t \in \mathcal{T} \setminus \{0\}, i \in \mathcal{U}$$
 (2)

$$\check{\mathcal{K}}_{v}^{t} = \bigcup_{u \in \mathcal{U}: \tau_{uv} = \tilde{t}} \mathcal{N}_{uv}^{t-\tilde{t}} \qquad \forall t \in \mathcal{T}, \tilde{t} \in \{0, 1, ..., t\}, v \in \mathcal{U} \tag{3}$$

$$\tilde{\mathcal{K}}_{u}^{t} = \hat{\mathcal{K}}_{u}^{t-\bar{W}} \qquad \forall t \in \mathcal{T}, u \in \mathcal{U}$$
 (4)

Based on the system dynamics elaborated above, we model this stochastic dynamic vehicle resource allocation problem as a Markov decision process (Xu et al., 2018b; Tang et al., 2020). Idle vehicle resource within each city is perceived as an agent because the vehicle assignment decisions are made for each city respectively. The components of this MDP formulation $M \triangleq < S_{\ell}\{A^{u}\}, P, R >$ are defined as follows.

States: The system state is captured by the tuple $\mathbf{S} = \{\mathbf{S}_h, \mathbf{S}_s, \mathbf{S}_d\}$. \mathbf{S}_h indicates the current horizon of a day. $\mathbf{S}_s = \{\mathbf{S}_s^u\}_{u \in \mathcal{U}} = \{((\varphi_{(0)}^{uv})_v, \varphi_0^u, \varphi_1^u, \varphi_2^u, \cdots \varphi_{\tau_s}^u)\}_{u \in \mathcal{U}}$ describes the supply states of available vehicle resource in each city. In the first term, φ_0^{uv} is the total number of empty seats in vehicles currently in service of line (u,v), the vector $(\varphi_{(0)}^{uv})_v$ describes currently available seat resources in different lines originating from city u without dispatching any vacant vehicle. $\varphi_i^u = |\mathcal{K}_u^{t+i}|$ is the accumulated number of vehicle resources for assignment in the future i-th horizon. $\mathbf{S}_d = \{\mathbf{S}_d^{uv}\}_{(u,v)\in\mathcal{L}} = \{(\omega_{(0)}^{uv},\omega_0^{uv},\hat{\omega}_1^{uv},\hat{\omega}_2^{uv},\cdots \hat{\omega}_{\tau_d}^{uv})\}_{(u,v)\in\mathcal{L}}$ describes the demand states in each line. $\omega_{(0)}^{uv}$ is the number of orders in line (u,v) that will expire if not served within the current horizon. ω_0^{uv} is the number of orders in the matching pool when making the dispatching decisions, while $\hat{\omega}_i^{uv}$ is the predicted number of newly emerging orders in line (u,v) in the future i-th horizon. The states not only specify the demand and supply information in the current horizon which will influence the instant reward but also describe the potential demand

and supply dynamics in several future horizons, which is helpful to capture the spatial-temporal demand and supply fluctuation. Notice that more detailed attributes of supply and demand, such as the specific locations of vehicles and orders, are not included in **S**, since we focus on approximating the effectiveness of resource allocation in the upper level of the framework and leave the evaluation of detailed information to the lower-level routing problem.

Actions: $\{A^u\}$ represents the joint action of all agents. In horizon t, the assignment decision of the idle fleet within city $u \in \mathcal{U}$ is a tuple $\mathbf{A}^u_t = ((|\mathcal{N}^t_{uv}|)_{v:(u,v)\in\mathcal{L}}, |\bar{\mathcal{K}}^t_u|)$, indicating the number of vehicles assigned to all lines originating from city u, and the number of vehicles reserved at the current city.

State transitions: The transition $(\mathbf{S}_t, \{\mathbf{A}_t^u\}, R_t, \mathbf{S}_{t+1})$ is a function of the selected action. During one transition, the dispatching action $\{\mathbf{A}^u\}$ is executed to update the subsequent system states. The next supply states are constructed following the constraints (1) to (4). The demand states are updated by the matching results within the current horizon and the newly emerging orders.

Rewards: The system reward function at horizon *t* is defined as follows.

$$R_t = \sum_{(u,v)\in\mathcal{L}} \left(\sum_{k\in\mathcal{N}_{uv}^t} R^{uv} s_k^t - \sum_{k\in\mathcal{N}_{uv}^t} C \delta_k^t - p_e R^{uv} \epsilon_{uv}^t \right)$$

The reward function is composed of three parts. The first part corresponds to the total revenue of vehicles dispatched at this horizon, where R^{uv} is the trip fare for a passenger and s_k^t is the number of passengers that vehicle k picked in this trip. The second part corresponds to the traveling costs caused by vehicles in \mathcal{N}_{uv}^t , where C denotes the cost per distance and δ_k^t is the total distance of this trip. The last part corresponds to the order lost penalty that occurred during this horizon, where p_e is the penalty rate for losing one passenger and ϵ_{uv}^t is the number of lost passengers in line (u,v). To calculate the reward value at each horizon, the number of matched orders s_k^t and the traveling distance are acquired. These values can be portrayed by solving the dynamic vehicle routing problems based on the available vehicle resources and demand information, which output the vehicle-order matching and the system profit of each line. Notice that in our framework, matching processes are executed more frequently to shorten the waiting time of passengers and vehicle routes may be adjusted in subsequent periods, s_k^t and δ_k^t are obtained by integrating the results of vehicle routing models within the next few horizons.

In the fleet dispatching problem, we seek to obtain a vehicle allocation policy π to maximize the expected discounted total rewards during the T horizons conditional on the initial states \mathbf{S}_0 . The overall objective function is shown as follows.

$$\max_{\pi} \mathbb{E}[\gamma^{t} \sum_{t=0}^{T-1} R_{t}(\mathbf{S}_{t}, \{\mathbf{A}_{t}^{u}\}) | \mathbf{S}_{0}]$$

For each horizon, the reward function $R_t(\mathbf{S}_t, \{\mathbf{A}_t^u\})$ is determined by solving the lower-level problem based on the decision \mathcal{N}_{uv}^t , which makes it difficult to solve the dynamic resource allocation problem embedded with dynamic DARP using model-based approximate dynamic programming approaches. It is also difficult to construct an explicit integrated mathematical model considering the heterogeneity of vehicles. Thus in this study, we take advantage of reinforcement learning techniques to tackle large-scale fleet dispatching problem. A more detailed description of our reinforcement learning algorithm is provided in subsection 4.1.

3.4 The vehicle routing model

The lower level problem optimizes the multi-vehicle pooled-ride routing problem for each line separately based on current orders in a greedy manner. The solution of dynamic DARP at each matching interval includes complete routes from the current location of each vehicle to the depot at the destination city. Thus routes planned at earlier periods can be updated to serve newly emerging orders. However, it is assumed that the vehicle-order matching obtained in earlier periods cannot be violated to avoid order loss. Vehicles travel along the routes at this matching interval and update their routes based on new routing results at the beginning of the next interval. This process is repeated at each matching interval to enable online vehicle routing in operations.

We formulate the online routing problem of line (u,v) in a matching interval at the dispatching horizon $t \in \mathcal{T}$ as a mixed-integer linear program (MILP). Let \mathcal{K}_{uv} denote the set of vehicles that are currently in a ride of this line, which also includes newly assigned vehicles \mathcal{N}_{uv}^t if this is the first matching after vehicle dispatching by the upper-level problem. The order set \mathcal{O}_{uv} includes all orders in the matching pool and the orders already matched by vehicles en route.

Let v_k be the location of vehicle $k \in \mathcal{K}_{uv}$ at the beginning of this matching interval. For order $p \in \mathcal{O}_{uv}$, the number of passengers is denoted as n_p , the origin is denoted as s_p with time window $[\mathring{L}_p, \mathring{U}_p]$, the destination is denoted as f_p with time window $[\mathring{L}_p, \mathring{U}_p]$. Notice that the vehicle-order matching obtained in earlier periods cannot be violated. Thus, orders in \mathcal{O}_{uv} can be classified into three categories. The first category \mathcal{O}_{uv}^1 are orders that have already been picked, and we use k_p to denote the vehicle that has served order p. The second category \mathcal{O}_{uv}^2 are orders that have already been matched but not picked, and we use k_p to denote the vehicle that has matched order p. The third category \mathcal{O}_{uv}^3 are orders still in the matching pool. Since orders in $\mathcal{O}_{uv}^1 \cup \mathcal{O}_{uv}^2$ have been matched in feasible routing solutions of the last few intervals, there must exist a feasible solution to complete the service of these orders at the current interval.

The routing problem is based on the complete graph $G(\mathcal{V}, \mathcal{A})$. The vertices $\mathcal{V} = \mathcal{V}_k \cup \mathcal{V}_f \cup \mathcal{V}_s \cup \{E\}$, where $\mathcal{V}_k = \{v_k, \forall k \in \mathcal{K}_{uv}\}$ indicates the locations of all vehicles at the beginning of the current interval, $\mathcal{V}_f = \{f_p, \forall p \in \mathcal{O}_{uv}\}$ indicates the destination nodes of all orders, $\mathcal{V}_s = \{s_p, \forall p \in \mathcal{O}_{uv}^2 \cup \mathcal{O}_{uv}^3\}$ indicates the origin nodes of the unserved orders, and E indicates the depot in the destination city. Let R^{uv} be the one-way trip fare on line (u, v), D_{ij} be the distance of arc (i, j), C be the travel cost per distance. The objective of the routing problem is to maximize the revenue of all vehicles, subtracted by traveling costs from their current locations to the depot in city v. The objective function is shown as follows.

$$\max \sum_{p \in \mathcal{O}_{uv}} \sum_{k \in \mathcal{K}_{uv}} R^{uv} n_p d_{pk} - C \sum_{(i,j) \in \mathcal{A}} \sum_{k \in \mathcal{K}_{uv}} y_{ij}^k D_{ij}$$

Decision variables in the vehicle routing model are given by x_{ij}^{pk} , y_{ij}^k , d_{pk} and u_{kj} . The first three variables are integer variables, where x_{ij}^{pk} indicates whether vehicle k passes arc (i,j) with passengers of order p, y_{ij}^k indicates whether vehicle k passes arc (i,j), d_{pk} indicates whether vehicle k serves order p, u_{kj} is a positive variable indicating the time for vehicle k to arrive at node j. The constraints can be formulated as follows.

$$\sum_{j \in \mathcal{V} \setminus \{i\}} \sum_{k \in \mathcal{K}_{uv}} y_{ij}^k \le 1$$
 $\forall i \in \mathcal{V}$ (5)

$$\sum_{j \in \mathcal{V} \setminus \{i\}} y_{ji}^k - \sum_{j' \in \mathcal{V} \setminus \{i\}} y_{ij'}^k = 0 \qquad \forall i \in \mathcal{V}_f \cup \mathcal{V}_s, k \in \mathcal{K}_{uv}$$
 (6)

$$\sum_{j \in \mathcal{V} \setminus \{v_k\}} y_{v_k j}^k = \sum_{j \in \mathcal{V} \setminus \{E\}} y_{jE}^k = 1 \qquad \forall k \in \mathcal{K}_{uv} \qquad (7)$$

$$d_{pk_n} = 1 \qquad \forall p \in \mathcal{O}_{uv}^1 \cup \mathcal{O}_{uv}^2 \qquad (8)$$

$$\sum_{k \in \mathcal{K}_{uv}} d_{pk} \le 1 \tag{9}$$

$$\sum_{j \in \mathcal{V} \setminus \{f_p\}} x_{jf_p}^{pk} - \sum_{j \in \mathcal{V} \setminus \{f_p\}} x_{f_p j}^{pk} = d_{pk} \qquad \forall p \in \mathcal{O}_{uv}, k \in \mathcal{K}_{uv} \qquad (10)$$

$$\sum_{j \in \mathcal{V} \setminus \{s_p\}} x_{s_p j}^{pk} - \sum_{j \in \mathcal{V} \setminus \{s_p\}} x_{j s_p}^{pk} = d_{pk} \qquad \forall p \in \mathcal{O}_{uv}^2 \cup \mathcal{O}_{uv}^3, k \in \mathcal{K}_{uv} \qquad (11)$$

$$\sum_{j \in \mathcal{V} \setminus \{i\}} x_{ij}^{pk} - \sum_{j' \in \mathcal{V} \setminus \{i\}} x_{j'i}^{pk} = 0 \qquad \forall p \in \mathcal{O}_{uv}, i \in \mathcal{V}_f \cup \mathcal{V}_s \setminus \{s_p, f_p\}, k \in \mathcal{K}_{uv}$$
 (12)

$$x_{ij}^{pk} \le y_{ij}^k \qquad \forall (i,j) \in \mathcal{A}, k \in \mathcal{K}_{uv} \qquad (13)$$

$$\sum_{p \in \mathcal{O}_{uv}} x_{ij}^{pk} n_p \le W y_{ij}^k \qquad \qquad \forall (i, j) \in \mathcal{A}, k \in \mathcal{K}_{uv} \qquad (14)$$

$$u_{kv_k} = t_0$$
 (15)

$$u_{kj} - u_{ki} \ge D_{ij}/s - M(1 - y_{ij}^k) \qquad \forall (i,j) \in \mathcal{A}, k \in \mathcal{K}_{uv} \qquad (16)$$

$$\hat{L}_p d_{pk} \le u_{kf_p} \le \hat{U}_p d_{pk} \qquad \forall p \in \mathcal{O}_{uv}, k \in \mathcal{K}_{uv} \qquad (18)$$

$$x_{ij}^{pk} \in \{0,1\}, y_{ij}^{k} \in \{0,1\}, d_{pk} \in \{0,1\}$$
 $\forall p \in \mathcal{O}_{uv}, (i,j) \in \mathcal{A}, k \in \mathcal{K}_{uv}$ (19)

Constraint (5) ensures that a vehicle originating from one node can reach at most one node, and each arc is passed by at most one vehicle. If more than two vehicles pass the same arc, there must exist a shorter route for one of them. Constraints (6) and (7) are flow conservation constraints that the route of any vehicle in \mathcal{K}_{uv} is continuous from its current location to the depot in city v. Constraints (8) and (9) indicate the matching between vehicles and orders. The matching of orders in \mathcal{O}_{uv}^1 and \mathcal{O}_{uv}^2 are determined before this matching interval, while each order in \mathcal{O}_{uv}^3 can be matched to at most one vehicle en route. Constraints from (10) to (13) represent that passengers are picked by the matched vehicle at the origin node and delivered to the destination. Constraint (14) ensures that the number of passengers in the vehicle will not exceed the capacity W. Constraints from (15) to (18) determine the time for vehicles to serve each node, where t_0 is the current time, which is the beginning of this matching interval, and M is a very large positive value in constraint (16). Based on the assumptions of hard time windows, vehicles have to serve the matched orders within the requested time windows. Vehicles may wait at the node if they arrive before the time window, while late arrivals lead to infeasible solutions.

The MILP formulation of the multi-vehicle pooled-ride routing problem is NP-hard. Since we have to solve this problem repeatedly at every matching interval, we leverage the ALNS heuristic to obtain a near-optimal solution efficiently. The detailed heuristic algorithm is introduced in subsection 4.2.

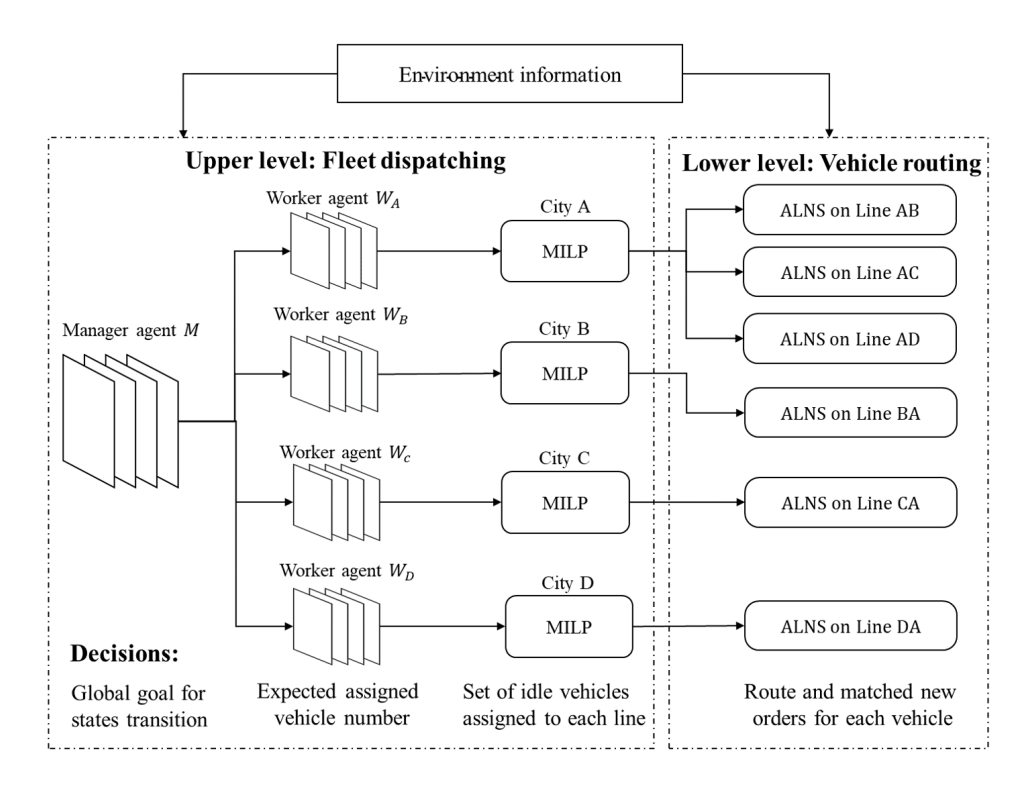


Figure 3: The fleet operational decision process for a network with one central city *A* and three surrounding cities *B*, *C*, and *D*.

4 Solution Methodologies

To tackle the challenges introduced in section 3, we propose a two-level reinforcement learning framework to implement dynamic fleet dispatching and online vehicle routing on intercity ridepooling services. A novel multi-agent hierarchical reinforcement learning method is adopted in the upper level of the framework to optimize the spatial-temporal allocation of vehicle resources by assigning idle vehicles to lines. The lower level of the framework uses ALNS heuristic to solve the proposed online multi-vehicle pooled-ride routing problem efficiently and effectively based on the assignment decision of the upper level.

Before delving into the specifics of the model, we provide an example that outlines the workflow across different levels of the framework. Consider the ride-pooling service provided in a city cluster with one central city *A* and three surrounding cities *B*, *C*, and *D*. Six intercity lines are available, including *AB*, *BA*, *AC*, *CA*, *AD* and *DA*. The corresponding operational decision process at the beginning of a dispatching horizon can be illustrated as shown in Figure 3.

Both levels of the framework observe distinct environmental information. The upper-level model focuses on assigning idle vehicles in each city to respective lines at the start of each horizon. To accomplish this, we employ MFuN to make dispatching decisions for each city, which consists of a manager-work hierarchical structure. The manager agent derives a goal as the direction for global state transitions, which is then conveyed to multiple worker agents. Each worker agent represents a city and determines the number of vehicles to assign to each line based on the manager's global state transition direction and its local observations. To account for the heterogeneity of the vehicles, a mixed integer linear program is executed independently for each

city, mapping the assigned vehicle numbers to the specific vehicle assignments.

The lower level of the framework addresses the online multi-vehicle pooled-ride routing problem as proposed in subsection 3.4 for each line separately at each matching interval. The first matching within each dispatching horizon incorporates the route planning of newly assigned vehicles obtained from the upper-level model. Subsequent matchings are performed based on the information of all vehicles en route. Then during the matching intervals, each vehicle can serve the matched orders following a sequence planned by the ALNS heuristic.

4.1 Upper level: Multi-agent feudal networks

The upper level of the framework is expected to learn the optimal vehicle dispatching policy for each city within the city cluster. In our study, idle vehicles within each city are regarded as an agent because the vehicle assignment is made for each city respectively. Since there are multiple cities in the city cluster, a group of agents has to operate collaboratively to improve the system throughput. Thus, we use a multi-agent reinforcement learning framework at the upper level. MARL has been widely used in fleet operations in ride-sourcing platforms, which performs well in scalability in large-scale problems (Xu et al., 2018a; Guo and Xu, 2020; Jiao et al., 2021; Kullman et al., 2022). However, MARL has a prominent drawback that the training process may be non-stationary when each agent updates its own policy. The system may fail to converge to the global optimum because each agent makes decisions based on its own utility function and local observation. Conventional reinforcement learning methods, such as Q-learning or policy gradient methods, usually exhibit high variance in multi-agent environments where coordination of agents is required (Lowe et al., 2017).

To handle the problem aroused by decentralized training, we propose a multi-agent feudal network framework to enhance dispatching decision coordination among agents in the intercity ride-pooling services. Feudal reinforcement learning (FRL) was first proposed by Dayan and Hinton (1992), Vezhnevets et al. (2017) introduced Feudal Networks (FuN) to extend conventional FRL to the form of the deep neural networks, which performs well in long timescale credit assignment, especially in environments with sparse reward signals. A manager module and a worker module are constructed in FuN, where the manager set goals as direction for the actions of the worker. The goals can be interpreted as an expected objective for global state transition in future periods. The worker receives intrinsic rewards for actions consistent with goals. Multiagent settings are introduced by Ahilan and Dayan (2019) to set multiple agents as workers. The shared goals can be used to encourage the cooperation of simultaneously-acting agents. This hierarchical framework is highly compatible with the fleet dispatching problem within the city cluster. The vehicle assignment decisions in each city are relatively independent during the current horizon, but the significant influence of these actions on the supply states of other agents propagates throughout the city network in subsequent periods, thereby influencing the overall system profit. Under the guidance of a global manager, all agents are expected to cooperate to improve the effectiveness of vehicle resource allocation to mitigate the imbalance between demand and supply.

4.1.1 Model structure

In this structure, we introduce the model structure of MFuN. This deep neural network system map states to actions as proposed in the MDP in section 3. The global state is captured by the

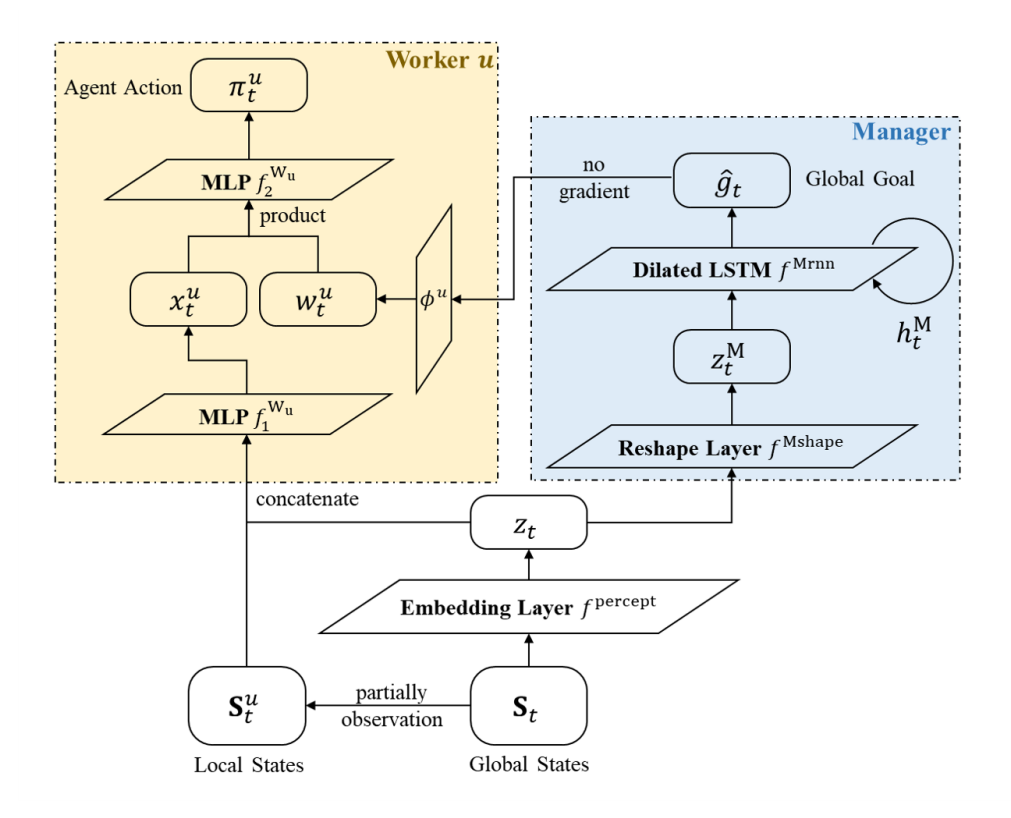


Figure 4: Structure of MFuN

tuple $\mathbf{S}_t = \{\mathbf{S}_h^t, \mathbf{S}_s^t, \mathbf{S}_d^t\}$, including the information of current horizon, supply in each city, and demand in each line. The action of each city \mathbf{A}_t^u is a tuple $((|\mathcal{N}_{uv}^t|)_{v:(u,v)\in\mathcal{L}}, |\bar{\mathcal{K}}_u^t|)$, indicating the number of idle vehicles assigned to all lines originating from this city, and the number of vehicles reserved.

We leverage multi-agent feudal networks as shown in Figure 4 to improve global coordination among the idle fleet of each city within the city cluster. The model contains a manager agent and several worker agents. The manager agent and worker agents share the embedding layer f^{percept} to obtain intermediate representation z_t based on global states \mathbf{S}_t . We use the same module for the manager agent M as proposed by Vezhnevets et al. (2017), which contains a reshape layer f^{Mshape} and a recurrent neural network architecture f^{Mrnn} . The output of the manager agent is a goal vector \hat{g}_t , which is obtained by a dilated LSTM model with input as reshaped z_t and internal states h_t^{M} . The dilated LSTM model is composed of r separate groups of sub-states, where r is a dilation radius. At time step t, only the t%r sub-states are updated, where % denotes the modulo operation, and the output is pooled across the previous c outputs to accomplish smooth variation. By updating only part of the whole states at each time, the dilated LSTM model can preserve the memories for longer periods without missing any input experience. The forward dynamics of the worker policy networks are given by Equations (20) and (21).

$$z_t^{\rm M} = f^{\rm Mshape}(z_t) \tag{20}$$

$$h_t^{\rm M}, \hat{g}_t = f^{\rm Mrnn}(z_t^{\rm M}, h_{t-1}^{\rm M})$$
 (21)

The module of a worker agent W_u is composed of two multi-layer perceptions (MLP) $f_1^{W_u}$ and $f_2^{W_u}$. Parameters in each worker module are not shared since they may differ in network scales.

The mathematical formulations of the worker policy networks are given by Equations (22), (23), and (24).

$$w_t^u = \phi^u(\sum_{i=t-c}^t g_i); g_t = \hat{g}_t / \|\hat{g}_t\|$$
 (22)

$$x_t^u = f_1^{\mathbf{W}_u}(z_t \oplus \mathbf{S}_t^u) \tag{23}$$

$$\pi_t^u = \operatorname{prob}(f_2^{W_u}(x_t^u w_t^u)) \tag{24}$$

For each worker agent W_u , the first MLP $f_1^{W_u}$ takes the concatenation of global state representation z_t and local observation \mathbf{S}_t^u as input. Here the local observation of agent W_u is composed of local supply and demand information. The local supply states are $\mathbf{S}_s^u = ((\varphi_{(0)}^{uv})_v, \varphi_0^u, \varphi_1^u, \varphi_2^u, \cdots \varphi_{\tau_s}^u)$, which include the number of currently available seat resources on the line originating from city u and idle vehicle resources at future horizons. The local demand states are $\{\mathbf{S}_d^{uv}\}_{(u,v)\in\mathcal{L}} = \{(\omega_{(0)}^{uv}, \omega_0^{uv}, \hat{\omega}_1^{uv}, \hat{\omega}_2^{uv}, \cdots \hat{\omega}_{\tau_d}^{uv})\}_{(u,v)\in\mathcal{L}}$, which summarizes the number of various unserved orders in each line originating from city u. Each worker agent is also influenced by the system goal g_t , which is a pooled summation of the last c goals proposed by the manager. The system goal is projected by an agent-specified linear transformation ϕ^u into a local goal vector w_t^u , which reflects the comprehension of goals by each agent based on their own features. The local goal vector is then combined with local intermediate representation x_t^u via product to output policy π_t^u .

Next, we introduce how to clarify the dispatching policy based on the output π_t^u . In the MDP proposed in subsection 3.3, the action of agent u is defined as $\mathbf{A}_t^u = ((|\mathcal{N}_{uv}^t|)_{v:(u,v)\in\mathcal{L}}, |\bar{\mathcal{K}}_u^t|)$, which is composed of $|\{v\}_{(u,v)\in\mathcal{L}}|+1$ dimensions, indicating the numbers of vehicles assigned to all lines originating from city u, and the number of vehicles reserved at the current city. In deep reinforcement learning problems with multidimensional action spaces, it is typically necessary for actions of different dimensions to be mutually independent. However, in the case of dispatching vehicles from a city, the number of vehicles dispatched to each city is not independent. The numbers of assigned vehicles are constrained by a summation equal to $|\mathcal{K}_u^t| = |\hat{\mathcal{K}}_u^t| + |\check{\mathcal{K}}_u^t| + |\bar{\mathcal{K}}_u^{t-1}| - |\tilde{\mathcal{K}}_u^t|$, which is the number of idle vehicles in the city. Hence, we cannot directly apply a common output layer, such as Softmax, in our neural networks. To address the interdependence between different dimensions in a single action A^{μ} , the actor networks of worker agents do not output the number of different assignments directly, they output the dispatching decisions of virtual vehicles instead. We create a set of V^u virtual vehicles to represent the available vehicles within \mathcal{K}_u^t . Each virtual vehicle selects a destination city from $|\mathbf{A}^u| = |\{v\}_{(u,v)\in\mathcal{L}}| + 1$ options, including city u and its neighbors, and the decisions of different virtual vehicles can be treated as mutually independent. Hence, the output of a worker agent π_t^u are in the form of the decisions of virtual vehicles, which is of $|\mathbf{A}^u| \times V^u$ dimensions as shown in Figure 5.

We can interpret the outputs in the form of multi-discrete decisions. Each element within π_t^u is a log-odds for this virtual vehicle choosing the corresponding dispatching option. These log-odds can be transformed into probabilities for sampling the actual actions as shown in Equation (24). By summing up the number of virtual vehicles that choose different destination cities, we can clarify the number of vehicles for each assignment. Decision masks are used to handle situations when the number of idle vehicles in reality is smaller than the predefined virtual list length V^u . In such cases, the actions of the last few virtual vehicles that cannot be mapped to realistic vehicles will be masked. If the number of idle vehicles in reality exceeds V^u , the excess vehicles will be kept in the current city at the current horizon.

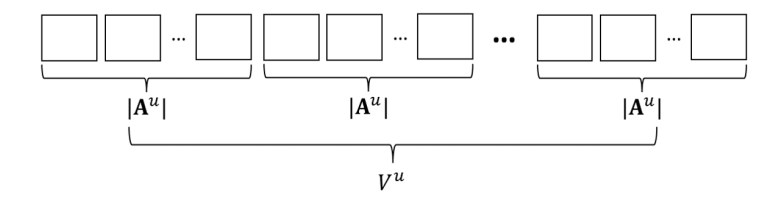


Figure 5: The output of worker agent *u*

4.1.2 Learning methods

We train the manager and workers with the Advantage Actor-Critic method, which learns the Actor function (the policy $\pi_{\theta}(\mathbf{S})$) and the Critic function $V_{\psi}(\mathbf{S})$ for all agents respectively. Many value-based learning methods, such as DQN and QMix, do not support multi-discrete decisions applied in our neural network, while the Advantage Actor-Critic method can still perform well.

At each iteration, we conduct a simulation of the daily operations of the intercity ridepooling services. The fleet dispatching decisions are made at each horizon to assign idle vehicles to lines in the simulation environment. After several iterations of interacting with the environment, we use batch gradient descent to update the policies of agents based on the transition experience of size $|\mathcal{B}|$. Let ψ^{M} and ψ^{W}_u be parameters in the critic networks of manager and worker u, θ^{M} and θ^{W}_u be parameters in actor networks of manager and worker u. The manager agent is trained as Equations (25), (26), and (27):

$$A_t^{M} = R_t + \gamma^{M} V_{\psi^{M}}(z_{t+1}) - V_{\psi^{M}}(z_t)$$
(25)

$$\mathcal{J}_{\psi^{\mathrm{M}}} = \frac{1}{2|\mathcal{B}|} \sum_{t \in \mathcal{B}} (A_t^{\mathrm{M}})^2 \tag{26}$$

$$\mathcal{J}_{\theta^{\mathrm{M}}} = -\frac{1}{|\mathcal{B}|} \sum_{t \in \mathcal{B}} A_t^{\mathrm{M}} \mathbf{d}_{\cos}(z_{t+c}^{\mathrm{M}} - z_t^{\mathrm{M}}, g_t(\theta^{\mathrm{M}}))$$
(27)

where $A_t^{\rm M}$ is the advantage function given the manager's immediate rewards R_t , which is the system reward function value defined in MDP, $\gamma^{\rm M}$ is a discount factor for the manager. We minimize the value loss function $\mathcal{J}_{\psi^{\rm M}}$ and policy loss function $\mathcal{J}_{\theta^{\rm M}}$ to update parameters of the critic and actor networks respectively. Here, policy loss is defined as the gap between actual state transitions in c steps and global goal in a cosine similarity manner. The worker agents are trained in a similar manner as Equations (28), (29), (30) and (31). The core difference is that a worker agent u is not only driven by its local immediate reward R_t^u but also encouraged by the intrinsic reward R_t^l to follow the goals. The local immediate reward of agent u is the profit of currently dispatched vehicles from the city u, subtracted by the penalty for order loss in the lines originating from city u. Similar to the system reward function R_t , the local rewards of each agent can be obtained by solving the routing problems in the simulation environment. The intrinsic reward, as shown in Equation (28), is the same for all workers, which represents the cooperation direction in global state spaces. The agents have to balance the trade-off between their rewards R_t^u and the shared objective. Then based on the experience trajectory, each worker is trained separately via minimizing the value loss function $\mathcal{I}_{\theta_v^{\rm M}}$ and policy loss function $\mathcal{I}_{\theta_v^{\rm M}}$.

$$R_t^I = \frac{1}{c} \sum_{i=1}^c d_{\cos}(z_t^M - z_{t-1}^M, g_{t-i})$$
 (28)

$$A_t^{W_u} = R_t^u + \alpha R_t^I + \gamma^W V_{\psi_u^W}(z_{t+1}, \mathbf{S}_{t+1}^u) - V_{\psi_u^W}(z_t, \mathbf{S}_t^u)$$
(29)

$$\mathcal{J}_{\psi_u^{W}} = \frac{1}{2|\mathcal{B}|} \sum_{t \in \mathcal{B}} (A_t^{W_u})^2 \tag{30}$$

$$\mathcal{J}_{\theta_u^{\mathcal{W}}} = -\frac{1}{|\mathcal{B}|} \sum_{t \in \mathcal{B}} A_t^{\mathcal{W}_u} \log(\pi_{t,\theta_u^{\mathcal{W}}}^u(z_t, S_t^u))$$
(31)

4.1.3 Determine vehicle assignment

The neural networks provide the number of vehicles assigned to each line and reserved in the current city, instead of providing dispatching decisions for each vehicle directly. Therefore, for each city, given the number of dispatching vehicles to different cities decided in MFuN, we have to decide the movement of each vehicle so that the number of dispatched vehicles in total is nearly consistent with \mathbf{A}^u . A MILP is proposed to map the numbers in \mathbf{A}^u into the sets of vehicles for each agent W_u respectively. Let \mathcal{E}_u be neighbors of the city u (including the city itself u), and a_v be the expected number of idle vehicles dispatched to the city $v \in \mathcal{E}_u$ obtained by the decisions of MFuN \mathbf{A}_u . Among all idle vehicles in the city u at dispatching horizon t, there may be some vehicles reaching maximum daily work time, which are expected to return to their original cities and get off work in time. Let \mathcal{F}_u^t be the set of vehicles that will be off duty in a few horizons. The objective function of the MILP includes three parts as mathematical expressions (32), (33), and (34).

$$p_1 = \sum_{v \in \mathcal{E}_v} \left| a_v - \sum_{k \in \mathcal{K}^t} x_{kv} \right| \tag{32}$$

$$p_2 = \sum_{v \in \mathcal{E}_u} \sum_{k \in \mathcal{F}_v^t} x_{kv} D_{vd_k} \tag{33}$$

$$p_3 = \sum_{k \in \mathcal{F}_u^t} \sum_{v \in \mathcal{E}_u \setminus \{u\}} x_{kv} \tilde{r}_k \tag{34}$$

where x_{kv} is a binary variable indicating whether vehicle k is dispatched to city v in this horizon. The mathematical expression (32) represents the gap between realistic assignment and actions of worker agent W_u . The mathematical expression (33) represents the total distances for all vehicles in \mathcal{F}_u^t to return origin cities after finishing the dispatched trip, where D_{vd_k} indicates the distance between city v and the origin city of vehicle k. Mathematical expression (34) is constructed from a fairness perspective, where \tilde{r}_k is a predefined parameter representing the reward for dispatching vehicle v to work rather than keep idling. The vehicles with a lower percentage of time spent in transit are set with larger \tilde{r}_k , these vehicles are given higher priority to be assigned to lines rather than being reserved in the city. Then the MILP can be formulated as follows.

$$\min \sum_{v \in \mathcal{E}_u} \beta_1 z_v + \beta_2 p_2 + \beta_3 p_3$$

$$s.t. \sum_{v \in \mathcal{E}_u} x_{kv} = 1 \qquad \forall k \in \mathcal{K}_u^t$$
 (35)

$$\sum_{v \in \mathcal{E}_u} D_{vd_k} x_{kv} \le D_{ud_k} \qquad \forall k \in \mathcal{F}_u^t \tag{36}$$

$$a_v - \sum_{k \in \mathcal{K}^t} x_{kv} \le z_v \qquad \forall v \in \mathcal{E}_u \tag{37}$$

$$-a_v + \sum_{k \in \mathcal{K}_u^t} x_{kv} \le z_v \qquad \forall v \in \mathcal{E}_u$$
 (38)

$$x_{kv} \in \{0, 1\} \qquad \forall v \in \mathcal{K}_u^t, v \in \mathcal{E}_u \tag{39}$$

The constraints include that each vehicle can only be dispatched to exactly one city, as shown in constraint (35), and that vehicle reaching maximum daily work time is not allowed to be dispatched to cities farther from its origin city, as shown in constraint (36). The objective function is a linear combination of mathematical expressions (32), (33) and (34). The design of weights β_1 , β_2 and β_3 first ensures that vehicles are dispatched consistently with the decisions of MFuN, and subsequently takes into account other factors. We linearize the absolute terms in (32) by introducing binary auxiliary variables z_v to constraints (37) and (38). This MILP can be solved quickly using commercial software.

We conclude this subsection with the pseudo-code in Algorithm 1, which shows the overall framework of training policies in a simulator.

Algorithm 1 Training process of MFuN

```
1: Initialize parameters \psi^{M}, \{\psi_{u}^{W}\}_{u}, \theta^{M} and \{\theta_{u}^{W}\}_{u};
2: for i = 1 \rightarrow \text{Iter do}
       Reset simulator and MFuN, observe initial states S_0;
4:
        for t = 0 \rightarrow T - 1 do
            Obtain \{\pi_t^u\} according to MFuN based on \mathbf{S}_t and hidden states;
5:
           Sample \{A_t^u\} based on \{\pi_t^u\} in the form of multi-discrete decisions;
6:
7:
           For each city, determine the assignment of each vehicle by solving the MILP proposed
   in subsection 4.1.3;
           Solve the vehicle routing problem for each line at each matching interval;
8:
           Receive rewards R_t, \{R_t^u\}_u and R_t^I, observe new environment states \mathbf{S}_{t+1}, reserve the
9:
    transition experience;
10:
       end for
       Calculate advantages based on Equations (25), (28), and (29);
11:
       Update parameters based on Equations (26), (27), (30), and (31).
12:
13: end for
```

4.2 Lower level: Adaptive large neighborhood search heuristic

Given idle vehicles assigned to a specific line, the routing problem can be solved at the beginning of each matching interval to generate a routing plan for each vehicle en route. Since the large-scale dynamic DARP formulation proposed in subsection 3.4 can not be solved by exact algorithms in an acceptable time, we use ALNS algorithm to obtain a near-optimal solution efficiently for online operations. ALNS is one of the most effective heuristic algorithms to solve multi-vehicle dial-a-ride problems, which is first proposed by Ropke and Pisinger (2006). Compared with conventional neighborhood search heuristics, ALNS uses various operators to enhance the movement in solution space. During each iteration of the search, a portion of orders in the current solution is removed by *removal operators* while some unfulfilled orders are inserted by *insertion operators* to construct a neighborhood solution. The choice of operators depends on the cumulative devotion to the objective function of each operator.

As in the proposed formulation, the ALNS algorithm is executed to obtain vehicle routes for each line separately at each time period. The inputs are the orders in the matching pool and information of all vehicles en route on this line, which also includes newly assigned vehicles at the first matching interval of each dispatching horizon. Information of order p contains the number of passengers n_p , coordinates and time windows of origin s_p and destination f_p . Information of vehicle k contains the current location v_k and information of orders already picked or matched. It is assumed that partially constructed routing plans in earlier periods are not allowed to be modified in subsequent periods, which is the same as the basic settings in subsection 3.1.

The neighborhood search process is initiated with a feasible solution. The initial routes are constructed based on the orders that have already been matched, following the sequence determined in earlier periods. Any unmatched orders are then inserted into the routes using the **Regret-2 method**. This method identifies the optimal position for inserting each order into each route. This is achieved by recursively evaluating all feasible positions given the order and the route. For each order, the difference between the profit obtained from the best insertion position and the second-best insertion position is calculated as the Regret-2 value. At each iteration, the order with the highest Regret-2 value is inserted into its best position, and the Regret-2 values for the remaining unmatched orders are updated for the subsequent insertions. This process continues until all feasible insertions have been completed.

One basic operation in ALNS is to evaluate the insertion of single order (both pickup and delivery nodes) into given feasible routes at the initialization stage and insertion stage. It is crucial to test the capacity feasibility and time window feasibility of an insertion, among which checking time window feasibility is extremely complex and time-consuming. We use the forward time slack method (FTS) to check the time window feasibility according to Gschwind and Drexl (2019), which can speed up the process obviously.

The neighborhood search process is embedded in a simulated annealing metaheuristic. The initial temperature is τ_0 , which decreases at each iteration as $\tau \leftarrow \tau \times c$, where c is the cooling rate. The neighborhood search process ends at the iteration with a temperature lower than the stopping temperature τ_e . ALNS learns over iterations which operators are more appropriate for the problem. Suppose there are *n* removal operators $\mathcal{R} = \{r_1, r_2, r_3, ... r_n\}$ and *m* insertion operators $\mathcal{I} = \{i_1, i_2, i_3, ... i_m\}$, where each operator is initialized with a score $s_o = 0$ and a weight $w_0 = 1$. At each iteration, the operator is selected probabilistically based on the operator weights. For example, the probability of removal operator r_i being selected is $P(r_i) = \frac{w_{r_i}}{\sum_{r_i \in \mathcal{R}} w_{r_i}}$. Let $F(\mathcal{S})$ be the objective function value of the current solution S, F(S') be the objective function value of the new solution S', $F(S^{\text{best}})$ be the objective function value of the historical best solution S^{best} . Suppose at a certain iteration, we choose operator $r_p \in \mathcal{R}$, $i_q \in \mathcal{I}$, then there exist four situations after the removal stage and insertion stage. The details of score updates are explained in pseudocode in Algorithm 2. The parameters are set as $\theta_1 > \theta_2 > \theta_3 > \theta_4$ such that operators leading to better solutions are enhanced adaptively in later stages. The weight of operator o is updated each iteration as $w_o \leftarrow (1-\alpha)w_o + \alpha \frac{s_o}{n_o}$, where n_o is the number of times operator o is used. The operator selection criteria reflect the flexible balance between exploration and exploitation throughout the iterations.

The operators used in our study are similar to Ghilas et al. (2016). The removal operators include:

(1)**Random removal operator**: randomly removes ϕ_r orders (both pickup and delivery nodes) from the solution.

Algorithm 2 Adaptive large neighborhood search heuristic

Input: Order information \mathcal{O}_{uv} , vehicle information \mathcal{K}_{uv} ; **Output:** Routing solution S; 1: Construct initial routing solution S, $S^{\text{best}} \leftarrow S$; 2: For each operator $o, s_o \leftarrow 0, w_o \leftarrow 1$; 3: $\tau \leftarrow \tau_0$; 4: while $\tau > \tau_e$ do For each operator o, $n_o \leftarrow 0$; **for** $j = 1 \rightarrow \text{Iter do}$ 6: 7: Choose removal operator $r \in \mathcal{R}$ and insertion operator $i \in \mathcal{I}$ based on weights; $S' \leftarrow i(r(S)), n_r \leftarrow n_r + 1, n_i \leftarrow n_i + 1;$ 8: if $F(S') > F(S^{\text{best}})$ then 9: $S^{\text{best}} \leftarrow S', S \leftarrow S', s_r \leftarrow s_r + \theta_1, s_i \leftarrow s_i + \theta_1;$ 10: else if $F(S^{\text{best}}) \ge F(S') > F(S)$ then 11: $\mathcal{S} \leftarrow \mathcal{S}', s_r \leftarrow s_r + \theta_2, s_i \leftarrow s_i + \theta_2;$ 12: else if $F(S') \leq F(S)$ then 13: Generate random variable $\epsilon \in [0, 1]$; 14: if $\epsilon \leq \exp(-\frac{F(S)-F(S')}{K\tau})$ then $S \leftarrow S', s_r \leftarrow s_r + \theta_3, s_i \leftarrow s_i + \theta_3$; 15: 16: else 17: $s_r \leftarrow s_r + \theta_4, s_i \leftarrow s_i + \theta_4;$ 18: 19: end if 20: 21: end for For each operator o, $w_o \leftarrow (1-\alpha)w_o + \alpha \frac{s_o}{n}$; 22: 23: $\tau \leftarrow \tau \times c$; 24: end while 25: return S^{best} .

- (2)**Shaw removal operator**: randomly removes 1 order, then remove $\phi_r 1$ orders that are similar in certain aspects, including the similarity of location and time window information.
 - (3)**Worst removal operator**: removes ϕ_r orders with the highest cost.
 - (4)**Time-based removal operator**: removes ϕ_r orders with the largest pick-up time delay.

The insertion operators include:

- (1)**Greedy insertion operator**: iteratively inserts an order (both pickup and delivery nodes) with the maximum additional objective function value to its best feasible position of the routes, until ϕ_i orders are inserted.
- (2)**Distance greedy insertion operator**: iteratively inserts an order with the shortest additional distance to its best feasible position of the routes, until ϕ_i orders are inserted.
- (3)**Regret**-m **insertion operator**: similar to the **Regret-2 method** introduced for initialization above, but insert orders with ϕ_i largest differences of profit between the best insertion position and the m-best insertion position.

5 Numerical Experiments

In this section, we conduct numerical experiments to verify the effectiveness of our proposed framework under different supply and demand scenarios based on three city networks, where the first two series of experiments are based on toy networks and the third series of experiments are based on realistic networks and operational data in Xiamen and its surrounding cities. All computational experiments are implemented on the computation platform with Intel(R) Core(TM) i5-12600KF CPU@3.70GHz 16GB RAM and RTX3070 (8GB) GPU. The algorithms are coded with Python 3.6. The neural network is constructed and trained with Pytorch. The mixed integer linear programs are solved by Gurobi 10.0.1.

A simulator is established to approximate the dynamics of intercity ride-pooling services, including the generation of orders and the operations of the vehicle fleet. Each vehicle starts working at a predetermined time and location. The system initially assigns vehicles to lines and then updates the routes of all vehicles in transit. Once vehicle dispatching and routing are executed, the states are updated accordingly. This procedure continues until the end of the operational time to complete a daily simulation. During the training process of the proposed reinforcement learning model, a full simulation of daily operations constitutes an episode of trajectory data for policy learning. To alleviate the computational burden and prevent memory overflow, we simplify the training process in the simulation environment in three ways. Firstly, during training iterations, the vehicle routing problem is only solved once after fleet dispatching in a horizon rather than solved at every matching interval. Vehicles travel along the planned route during the horizon without intermediate route updating until the next assignment of idle vehicles. This simplification is reasonable when the newly emerging orders within a dispatching horizon are assumed to be known at the first matching process. Secondly, during the training process, only a few iterations are performed in ALNS to solve the multi-vehicle routing problem based on the initial solution. This approach reduces the training time since ALNS need to be repeatedly solved in the simulation. Thirdly, the vehicle routing problem is based on the Euclidean metric in both the toy network and the realistic network. We calibrate the detour ratio in the realistic network using trajectory data from operations to approximate the travel distances in reality.

To better evaluate the effectiveness of the proposed MFuN framework, we introduce a myopic strategy and several reinforcement learning methods for the upper-level problem as benchmarks. The myopic method optimizes dispatching decisions based on the current supply and demand states. It determines the number of vehicles assigned to each line by considering the number of orders in the matching pool of the corresponding line. If the total number of idle vehicles within a city is sufficient to fulfill the assignment, vehicles are randomly assigned to lines as planned, while the remaining vehicles are reserved for the next dispatching. However, if there are not enough idle vehicles available for assignment, vehicles assigned to each line are distributed proportionally based on the number of vehicles needed to match the unserved orders. The myopic method also uses ALNS to solve the vehicle routing problem at the lower level of the framework. We also use several RL methods as benchmarks to show the advantage of MFuN in training. The details of these RL methods and their performances are presented in subsection 5.1. In subsections 5.2, 5.3, and 5.4, our main focus is to compare the optimization performance of the proposed MFuN framework with the myopic method, because the myopic method exhibits strong interpretability compared to RL methods, which can clearly demonstrate the impact of decision-making based on the current states.

The evaluation of the proposed methods will be based on several key indices, including the average daily profit and the order fulfillment ratio. In the context of intercity passenger transportation, the platforms also emphasize the vehicle utilization rate, which represents the percentage of time vehicles spend in transit. In the subsequent sections, we will compare the performance of different methods based on these indices. This comparative analysis aims to evaluate the system's overall performance and illustrate the specific characteristics and properties of each method.

5.1 Learning curves

We first focus on the training process of the reinforcement learning method at the upper level of the framework. All algorithms are trained over 3000 episodes. Each episode contains 44 time steps in toy networks and 60 time steps in realistic networks, where a step represents a dispatching horizon of 20 minutes in simulation. In MFuN, we set $\gamma^M = 0.99$ for the manager agent and $\gamma^W = 0.95$ for worker agents. We use RMSprop optimizer for manager and workers with a learning rate of the policy optimizer as 2.5×10^{-4} . The reward function $R_t = \sum_{(u,v) \in \mathcal{L}} (\sum_{k \in \mathcal{N}_{uv}^t} R^{uv} s_k^t - \sum_{k \in \mathcal{N}_{uv}^t} C \delta_k^t - p_e R^{uv} \epsilon_{uv}^t)$, where p_e is set to be 0.5 in all experiments. These parameters are used in training policies for algorithms under all scenarios in subsequent sections.

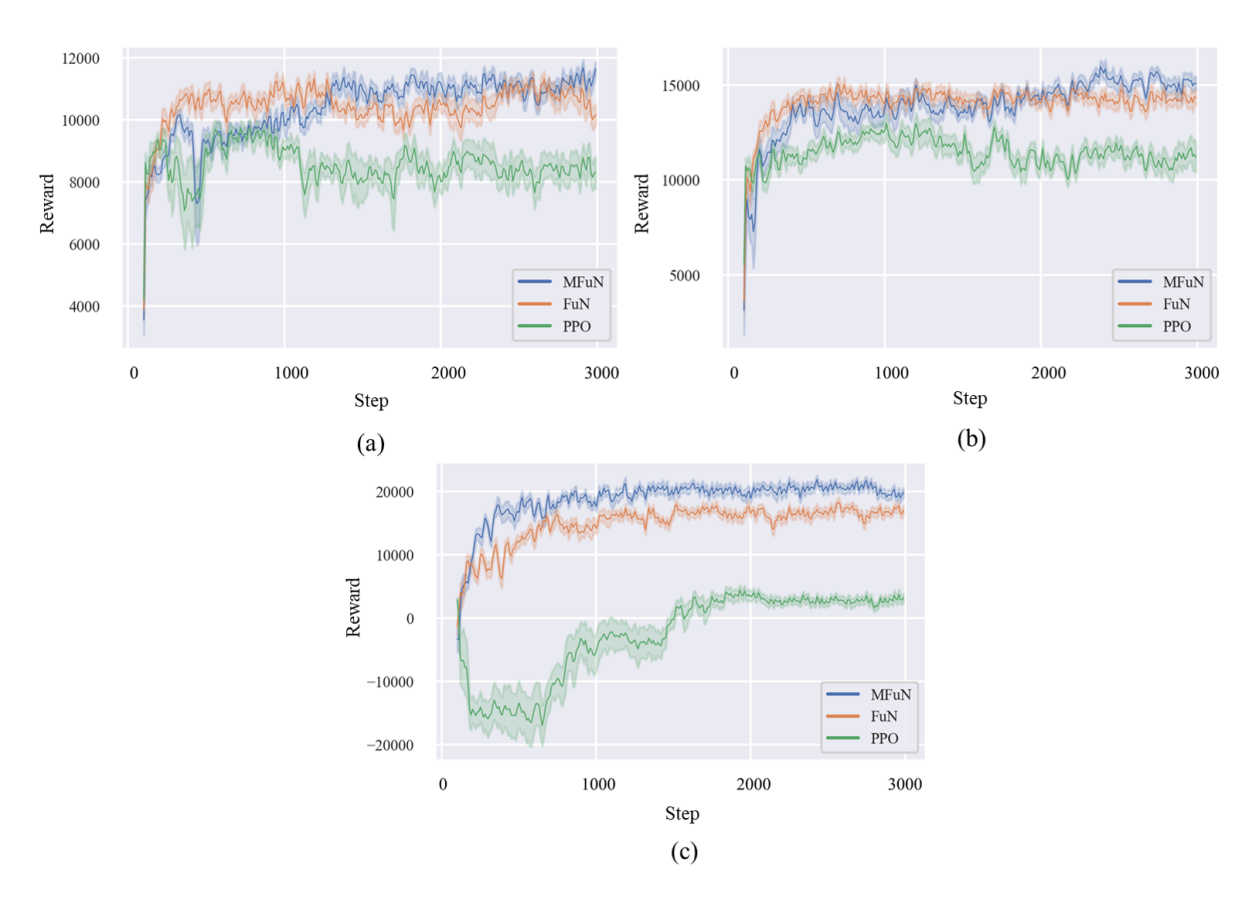


Figure 6: Learning curves of different RL methods in different networks. (a) The 2-city-2-line toy network. (b) The 3-city-4-line toy network. (c) Realistic network.

To validate the learning effectiveness of our multi-agent feudal networks, we compare our proposed framework with other RL methods employed as the upper-level model. The first benchmark method is the centralized decision feudal networks (FuN) based on the Advantage Actor-Critic method. This model consists of a single manager and a single worker, which jointly generate the dispatching decisions for all cities. The second benchmark method uses a multi-layer perceptron as the network and trains the model by the Proximal Policy Optimization algorithm (PPO). This model also makes centralized decisions in a multi-discrete manner. The output of neural networks in FuN and PPO is similar to the output in MFuN, which is the number of vehicles assigned to each line and reserved in the current city, the difference is that MFuN provides the numbers of vehicle allocation for each city respectively through different worker agents, while FuN and PPO derive the number of assignment in all cities as a vector. The movement of each vehicle is then determined as in subsection 4.1.3. By comparing our proposed MFuN framework with these benchmark methods, we aim to assess its advantages in learning an intelligent policy in the stochastic dynamic vehicle resource allocation problem.

Figure 6(a) and (b) show the learning curves of the models on relatively small networks, which contain only 2 and 4 lines respectively. The blue curves represent the reward obtained by the MFuN method over episodes, and the red and green curves represent the FuN method and PPO method respectively. Benefiting from the guidance of hierarchical reinforcement learning, the training results of MFuN and FuN are significantly more stable than PPO. The results of MFuN and FuN are basically similar in this example, however, the advantage of multi-agent decision becomes more obvious when the network complexity increases. Figure 6(c) shows the learning curve on a realistic network with 7 cities and 12 lines. Compared with smaller network, the advantage of hierarchical reinforcement learning over the fully connected network is more pronounced. The learning curves of PPO exhibit dramatic fluctuations, indicating that the training process of the hierarchical framework is more stable. In contrast, MFuN achieves a higher daily profit compared to FuN, particularly as the number of agents increases. This highlights that the centralized decision framework is significantly influenced by the large joint action space for the worker agent. The advantage of MARL becomes evident in terms of scalability. Each agent learns its own policy, allowing for better performance as the number of agents grows. On the other hand, centralized decision approaches tend to exhibit relatively poor performance when the joint action space of agents expands exponentially. The learning curves obtained from experiments with different network scales further demonstrate the proficiency of MFuN in longterm credit assignment and multi-agent cooperation. It excels in effectively handling complex scenarios and promoting efficient coordination among agents.

5.2 A 2-city-2-line toy network

The 2-city-2-line toy network is the simplest and most basic intercity transportation network. Numerical experiments based on this network are able to demonstrate the effectiveness of the proposed framework on **temporal scheduling**. The dispatching decisions in the 2-city-2-line toy network illustrate how various methods adapt to fluctuations in supply and demand by only adjusting the departure time of each vehicle. Figure 7(a) depicts the network topology of two cities, which have a radius of 15 and the distance between two cities is 60. Vehicle speed is 1 and traveling cost *C* is 1 per unit of distance. Figure 7(b) portrays the demand of two lines. Line 1, which runs from city A to city B, experiences a steady demand flow throughout the experiment. On the other hand, line 2, which operates from city B to city A, exhibits time-heterogeneous demand patterns. Specifically, there is a demand peak lasting for 200 minutes, four times higher

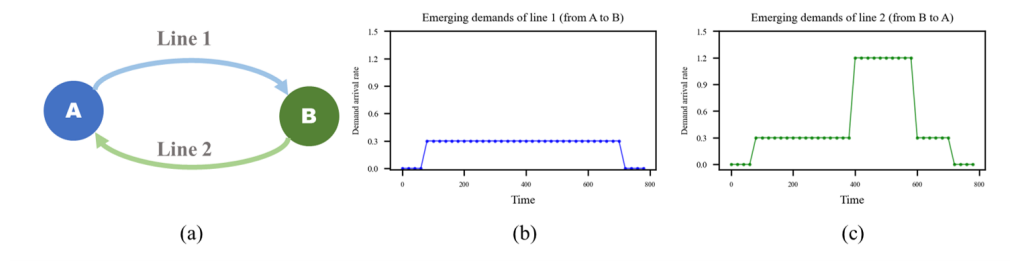


Figure 7: A 2-city-2-line toy network. (a) Topology of the network. (b) Demand from city A to B. (c) Demand from city B to A.

than the demand during low-demand periods. To simulate the dynamics of the ride-pooling service, we set the time window for picking up passengers as a normal distribution with a mean of 80 minutes. Additionally, the reservation lead time is modeled as a normal distribution with a mean of 40 minutes. In this series of experiments, a fleet consisting of 20 homogeneous 7-seat vehicles is utilized. The vehicles start their operations in city A at the initial moment and are available for serving ride requests throughout the simulation.

5.2.1 Sensitivity analysis of trip fare

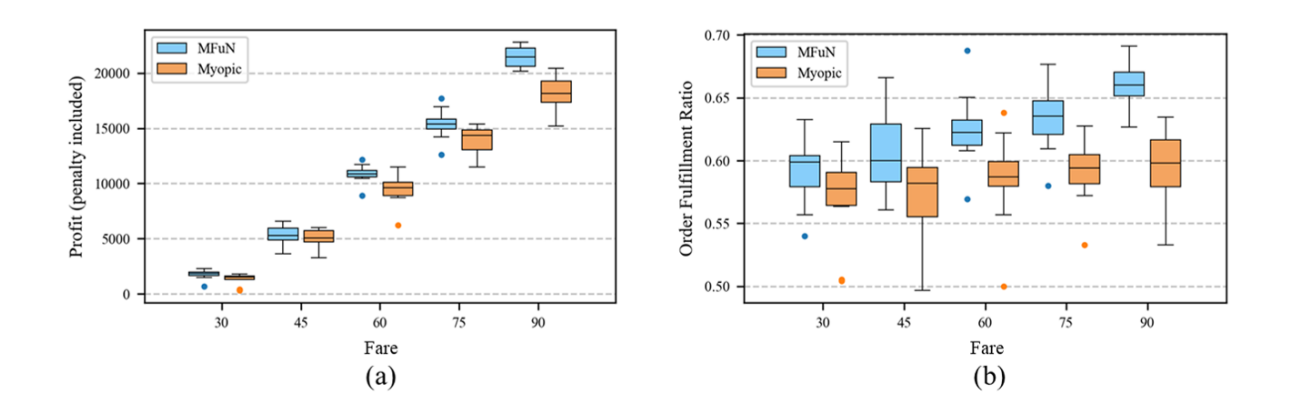


Figure 8: Performance of MFuN and Myopic in the 2-city-2-line toy network under different trip fares. (a) Profit. (b) Order fulfillment ratio.

In this subsection, we examine the impact of the one-way pooled-ride trip fare on the vehicle dispatching strategy. We set $R^{AB}=R^{BA}$, which means the trip fares of both lines are the same. We vary this trip fare values to be 30, 45, 60, 75, and 90 for each passenger. Considering that the one-way traveling cost is at least 60, it means that a vehicle must transport at least two passengers to achieve profitability when the trip fare is relatively low. However, as the trip fare increases, the condition for vehicle profitability with respect to the occupancy rate becomes less stringent, enabling more flexible dispatching strategies.

As depicted in Figure 8, it can be observed that the Myopic method exhibits little sensitivity to changes in trip fare. Under this method, the one-way trip fare does not directly influence the dispatching schedule of vehicles. However, it does impact vehicle routing, as higher trip fares encourage picking up more passengers with longer detour distances within the city. Consequently,

this leads to a slight increase in the order fulfillment ratio. In contrast, the MFuN framework demonstrates more intelligent vehicle scheduling. It consistently achieves higher daily profits and order fulfillment ratios compared to the Myopic method across various trip fare settings. Additionally, the increase in trip fare has a more pronounced positive impact on MFuN, particularly in improving the order fulfillment ratio. Under the high trip fare scenarios, MFuN achieves a significant improvement of 16.8% in the order fulfillment ratio during demand peak periods, and a 7.1% improvement in the daily average order fulfillment ratio, compared to the Myopic method.

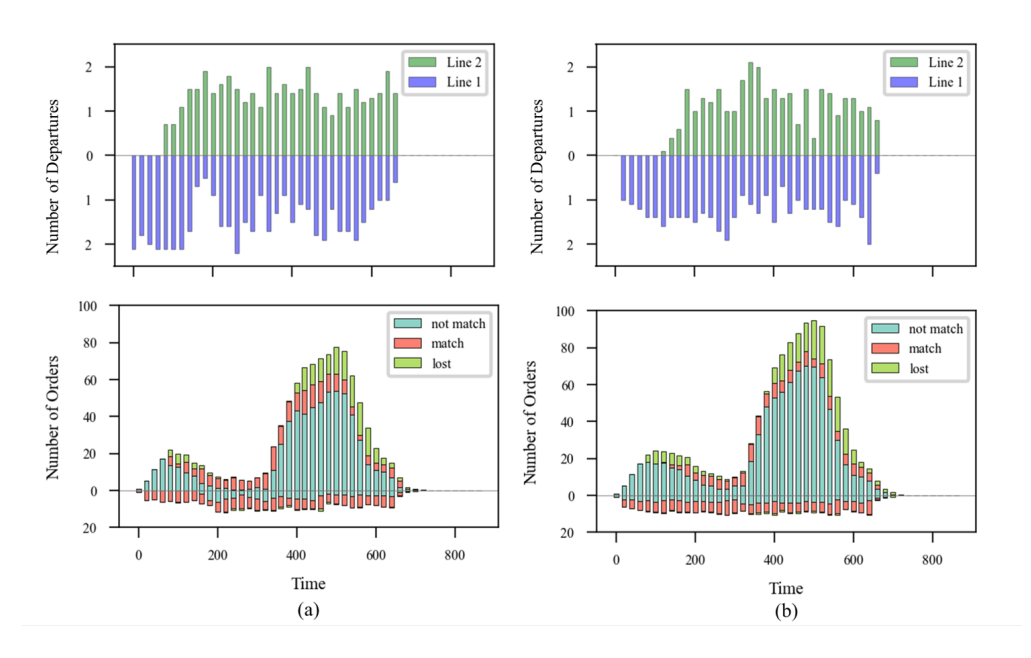


Figure 9: Number of departures and orders in each period. (a) MFuN. (b) Myopic.

To further illustrate the MFuN optimization mechanism, Figure 9 shows the average number of departures and order fulfillment during each time interval at a trip fare of 60. Figure 9(a) illustrates the vehicle dispatching pattern under the MFuN framework, while Figure 9(b) represents the dispatching approach of the myopic method. The upper figures show the average number of departures of idle vehicles at both lines at each horizon. The lower figures show the average number of lost orders (green), matched orders (red), and the orders not matched in this horizon but still available (cyan), these unmatched orders are still in the matching pool for batch-matching in the next dispatching horizon. In the early stages of the day, the MFuN framework dispatches a larger number of vehicles from city A to city B, even when both lines are experiencing low demand. This proactive dispatching strategy ensures that there are sufficient vehicle resources available in city B ahead of time, thereby minimizing the potential for order loss. Between 200 and 260 minutes, some vehicles have already completed a round trip and are dispatched back to city B in anticipation of the potential demand peak. Under the MFuN framework, more vehicles arrive in city B during the demand peak compared to the myopic method. The proactive vehicle dispatching employed by the MFuN framework allows for serving more passengers during the demand peak, thereby reducing customer waiting time and enhancing the overall passenger experience to a certain extent.

5.2.2 Sensitivity analysis of the distances between cities

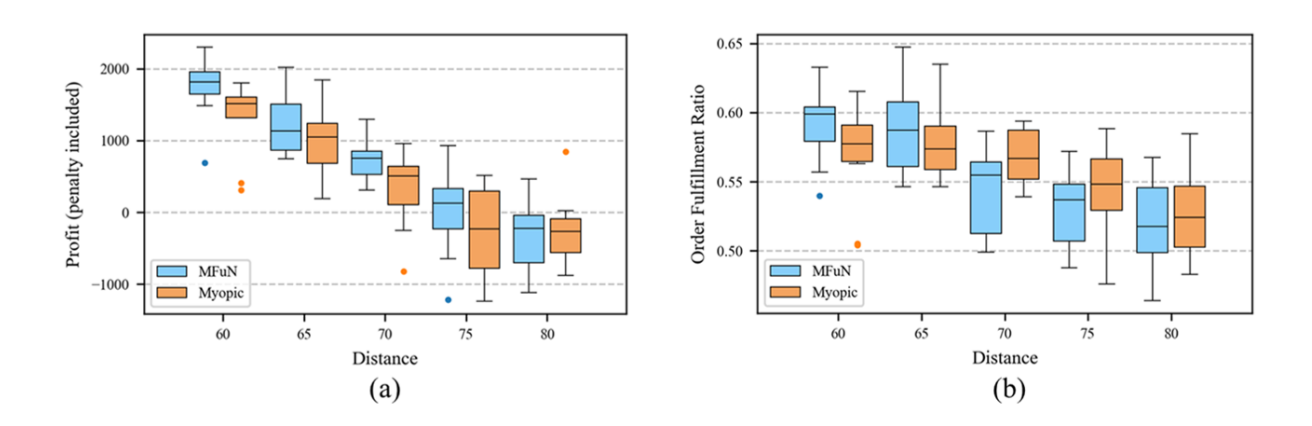


Figure 10: Performance of MFuN and Myopic in the 2-city-2-line toy network under different inter-city distances. (a) Profit. (b) Order fulfillment ratio.

In this subsection, we focus on the differences in dispatching strategies under different intercity distances, ranging from 60 to 80, while keeping the one-way trip fare fixed at 30. Considering a one-way trip fare of 30 and an inter-city distance of 60 to 80, a vehicle must carry at least 2 to 3 passengers on a one-way trip to avoid losses. As depicted in Figure 10, both the average daily profit and the order fulfillment ratio gradually decline as the distance between cities increases, regardless of the method employed. However, the MFuN approach demonstrates advantages in terms of profit in all scenarios, although it exhibits a lower order fulfillment ratio in cases where the distance is relatively large. The MFuN framework aims to enhance overall system profitability by increasing the average number of passengers per trip, even if it means some orders may not be served due to a more conservative dispatching strategy. Furthermore, when the distance between cities is large, MFuN optimally utilizes the abundant demand during peak periods. This accumulation of vehicle resources in advance allows for a higher occupancy rate during peak periods, leading to improved efficiency. In contrast to subsection 5.2.1, where MFuN intensifies the frequency of departures to serve more orders in scenarios with high trip fares, in situations with a relatively large inter-city distance, MFuN reduces the frequency of departures to enhance one-way profitability. This showcases the MFuN framework's ability to propose diverse and efficient dispatching strategies tailored to different demand and supply scenarios.

5.3 A 3-city-4-line toy network

The 3-city-4-line toy network contains one central city (A) and two neighboring cities (B, C). At the beginning of each horizon, the idle vehicles in the central city can be assigned to lines to any of the neighboring cities immediately or continue to wait for the next dispatching. Compared to experiments conducted in the 2-city-2-line network in subsection 5.2, this subsection is devoted to demonstrating the effectiveness of the proposed framework on **spatially allocating** vehicle resources. Figure 11(a) depicts the network topology, where the distance from city A to city B and C is both 60. The blue lines are line 1 and line 3 originating from city A, while the green and orange lines originate from city B and C respectively. Figure 11(b) depicts the demand fluctuation on four lines. Among the four lines, there exists a demand peak during the evening periods from

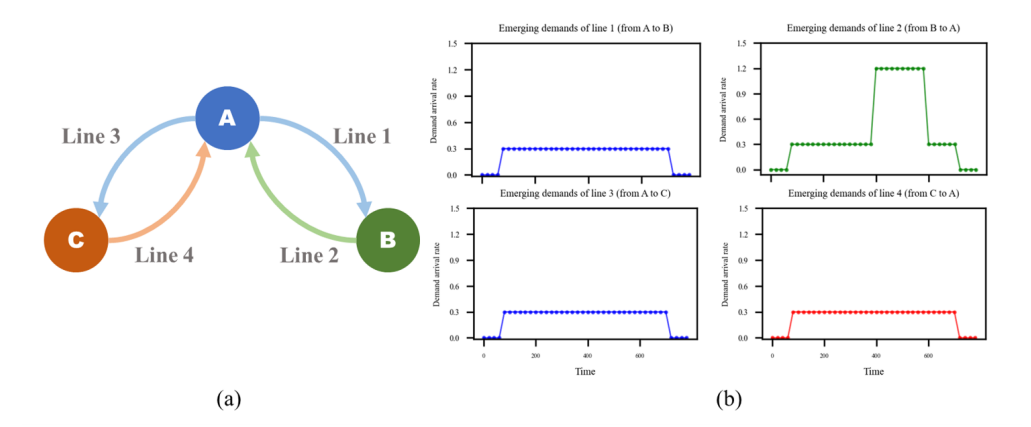


Figure 11: The 3-city-4-line toy network. (a) Topology of the network. (b) Demand of all lines.

city B to city A, while the other three lines are of relatively low demand throughout the day. A fleet of 30 homogeneous vehicles is considered in this series of experiments. Other basic settings are consistent with subsection 5.2.

Based on the network topology shown in Figure 11(a), we design 5 supply and demand scenarios to evaluate the spatial resource allocation performance, including: (1) all vehicles are initially located at city A with demands demonstrated in Figure 11(b); (2) all vehicles are initially located at city A. There also exists a demand peak on line 4 based on demands demonstrated in Figure 11(b), but the intensity is half of the demand peak on line 2; (3) all vehicles are initially located in city A. The demand fluctuation is based on demands in scenario (2) while the demand peak occurs at the same time on lines 1 and 3 instead of lines 2 and 4; (4) the demand scenario is the same as Figure 11(b), while all vehicles are initially located at city B; (5) the demand scenario is the same as Figure 11(b), while all vehicles are initially evenly distributed in three cities.

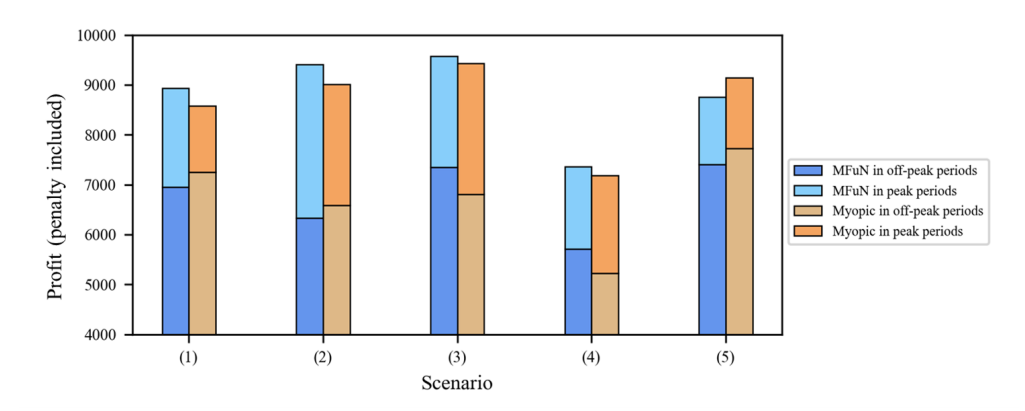


Figure 12: Daily profit in the 3-city-4-line toy network under five demand and supply scenarios.

Figures 12 and 13 illustrate the average daily profit and the average number of fulfilled orders under various scenarios. The daily revenue of MFuN is relatively higher than the values of myopic among the most supply and demand scenarios, basically attaining 3% to 7% improvement compared to the myopic method. MFuN also maintains a relatively satisfactory order fulfillment ratio.

However, the optimization mechanism differs across the five scenarios. Under scenarios (1)

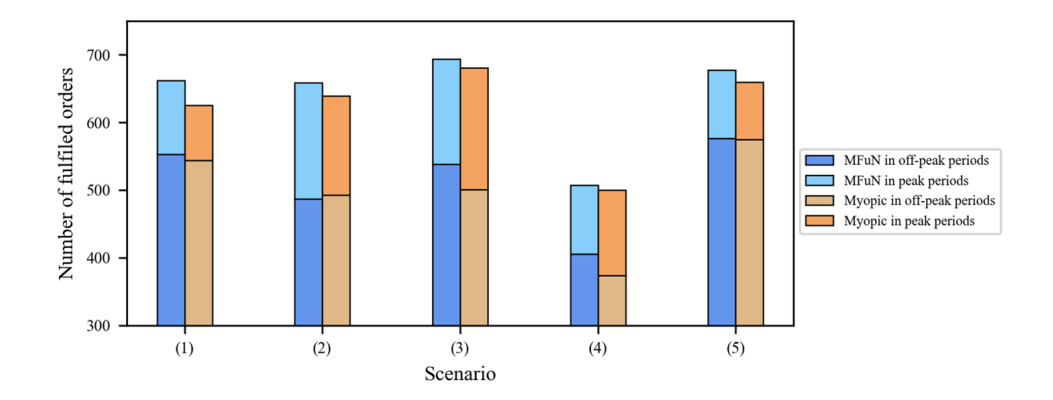


Figure 13: Number of fulfilled orders in the 3-city-4-line toy network under five demand and supply scenarios.

and (2), the advantage of MFuN is mainly reflected in serving more orders during high-demand periods. The MFuN framework dispatches more vehicles to city B compared to city C before and during the peak periods, which is the origination of the high-demand line. Prior to and during peak periods, the MFuN framework dispatches a larger number of vehicles to city B, which is the origin of the high-demand line. This allocation strategy of vehicle resources has a slight impact on service capacity during off-peak periods but ensures a relatively abundant availability of vehicles during the demand peak. There are 17% more vehicle departures from city B to fulfill over 20% more orders in high-demand lines during the peak periods under the dispatching of MFuN framework compared to myopic method.

In scenarios (3) and (4), the advantage of the MFuN framework during peak periods is less apparent. However, MFuN excels in providing more services primarily in low-demand lines during off-peak periods, leading to improved daily profits. This is primarily attributed to the demand peak under scenarios (3) and (4) occurring on lines originating from cities where vehicles are initially concentrated. Under the dispatching strategy of the myopic method, fleet operations are insufficient in the early periods of the day. As a result, a certain number of idle vehicles accumulate at the initial city during low-demand periods before the peak demand emerges. In contrast, the MFuN framework proactively dispatches more vehicles to the neighboring cities in the early stages, which exhibits more advantages in terms of fulfilling orders in low-demand lines during the off-peak periods.

Additionally, when vehicles are evenly distributed initially under scenario (5), no significant advantages are observed for the performance of the MFuN strategies compared to the myopic method. In this particular scenario, MFuN incurs higher traveling costs, resulting in slightly lower overall profits compared to the myopic method.

This series of experiments highlights that the optimization effect of the MFuN framework lies primarily in its ability to exploit flexible vehicle resource allocation to mitigate spatial imbalances between supply and demand. The MFuN framework excels in scenarios where there is a significant imbalance between the demand on a specific line and the supply in its originating city, such as during peak periods in scenarios (1) and (2). In these cases, MFuN demonstrates clear advantages in efficiently dispatching fleets to mitigate the effects of supply shortages. However, in other scenarios, the advantages of the MFuN framework become less apparent due to the relatively balanced supply and demand conditions. These results highlight the adaptability of

the MFuN framework to address spatial imbalances and effectively allocate resources where they are most needed. By strategically dispatching vehicles and optimizing fleet operations, MFuN can mitigate the negative impacts of supply shortages and enhance the overall performance of intercity ride-pooling services.

5.4 Realistic network

After verifying the effectiveness of the proposed framework from the perspective of temporally vehicle scheduling and spatial fleet allocation in subsection 5.2 and 5.3 respectively, we conduct numerical experiments based on a realistic network of Xiamen and its surrounding cities in this subsection. The Xiamen city cluster is situated on the southeast coast of China. The core urban area, Xiamen Island, has a developed economy and thriving market, which is closely interconnected with surrounding cities, forming a network of transportation and economic activities. For our study, we obtain the operational data from an intercity ride-pooling platform operating in Xiamen during the months of June and July 2022. The dataset encompasses information from 130,112 orders across 12 different lines connecting Xiamen with six surrounding cities. The surrounding cities vary in the distance to Xiamen Island. The city farthest from Xiamen is Xianyou, which is 169 kilometers away, while the nearest city Longhai is only 37 kilometers away. To cater to the intercity travel demands within the city cluster, a fleet of 291 vehicles is deployed and operated for intercity ride-pooling services in reality. Figure 14 shows the distribution of origins and destinations of all intercity ride-pooling orders within an hour in the operational data.

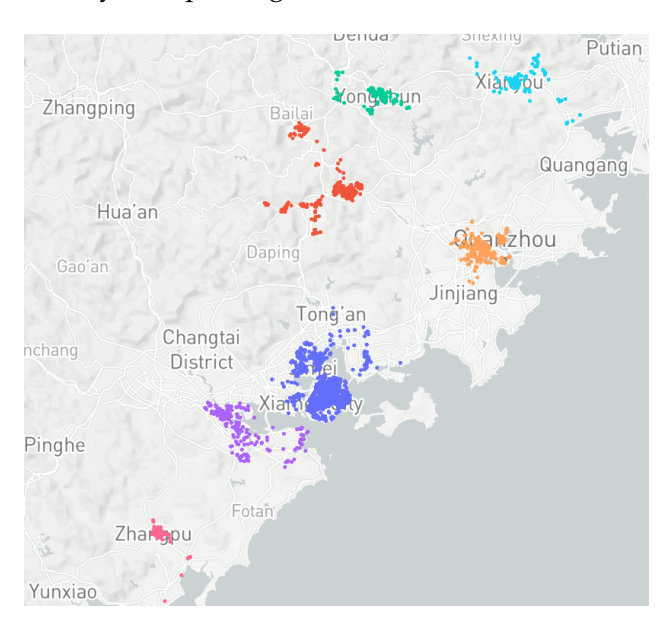


Figure 14: Distribution of realistic demand origins and destinations within an hour.

In this subsection, we replicate the realistic operational settings by utilizing a simulator, and we also generate the training dataset based on the passenger behavior observed in the realistic demand data by employing several data-driven techniques. First, we calculate the average intensity of newly emerging demands for each line within every 10 minutes, based on the realistic demand data. Using these parameters, we generate demand in the training data by modeling it as a non-homogeneous Poisson process. To determine the locations of the orders in the training data, we project the latitude and longitude of each order's origin and destination from the

realistic data into Cartesian coordinates, based on which we generate the locations of orders in the training dataset. The travel time between origin and destination is calculated using the Euclidean distance metric. However, to account for the detouring behavior observed in the operational data, we calibrate the detour ratio in urban areas and on intercity roads respectively based on trajectory data. This adjustment ensures that the simulated travel times reflect the real-world detouring patterns. Additionally, we generate a hard time window for picking each order. The width of the pickup time window follows a normal distribution with a mean of 60 minutes. To ensure a satisfactory passenger experience and avoid excessive detours, we set a maximum allowable arrival time for each order.

The one-way pooled-ride trip fare of each line in the simulator is consistent with the average level in reality, ranging from 35 to 100 for different lines. The traveling cost C is 0.5 per kilometer. The maximum daily work time for each vehicle \bar{W} is 10 hours, and the vehicles have to take a rest of 20 minutes after an intercity trip for safety considerations. The daily simulation begins at 3:00 am and lasts for 60 steps with each time step representing a dispatching horizon of 20 minutes.

5.4.1 Performance under different demand and supply scenarios

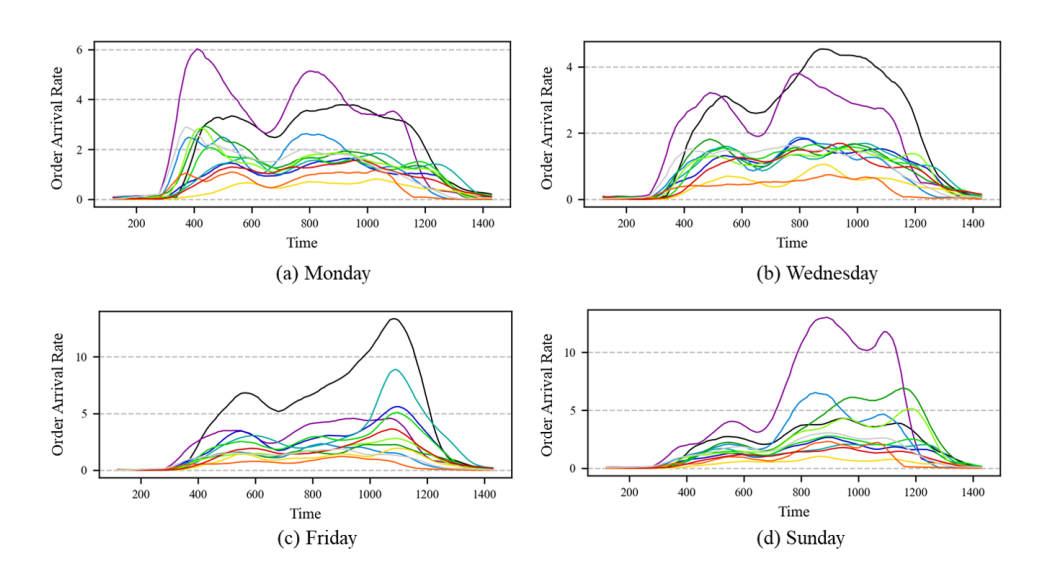


Figure 15: Daily fluctuation of demand for each line. (a) Monday. (b) Wednesday. (c) Friday. (d) Sunday.

Intercity travel demand within the city cluster exhibits noticeable periodicity, as observed in the realistic operational data. The data reveals that the demand for each line follows a weekly cycle, with consistent patterns on the same weekday across different weeks. Figure 15 illustrates the daily fluctuations of emerging orders per 10 minutes for 12 lines on Monday, Wednesday, Friday, and Sunday. For each week, there is a substantial demand from surrounding cities to the central city on Sunday afternoons and early Monday mornings. Conversely, on Friday afternoons, there is an almost equal amount of demand from the central city to surrounding cities. There also exists demand peaks in the morning and evening of each day, although these peaks have lower intensity compared to the weekly fluctuation pattern. Furthermore, it's worth noting that the demand varies in scale across different lines, as shown by different lines in Figure 15. The

complex demand patterns contribute to significant spatiotemporal variations in both demand and supply. The ride-pooling platform must intelligently allocate vehicle resources among the lines and optimize the matching of supply and demand through flexible scheduling, taking into account the specific temporal characteristics of the demand patterns. We train models for fleet operations under the demand scenarios of four different weekdays respectively to illustrate the effectiveness of the proposed MFuN framework, as shown in Figure 16.

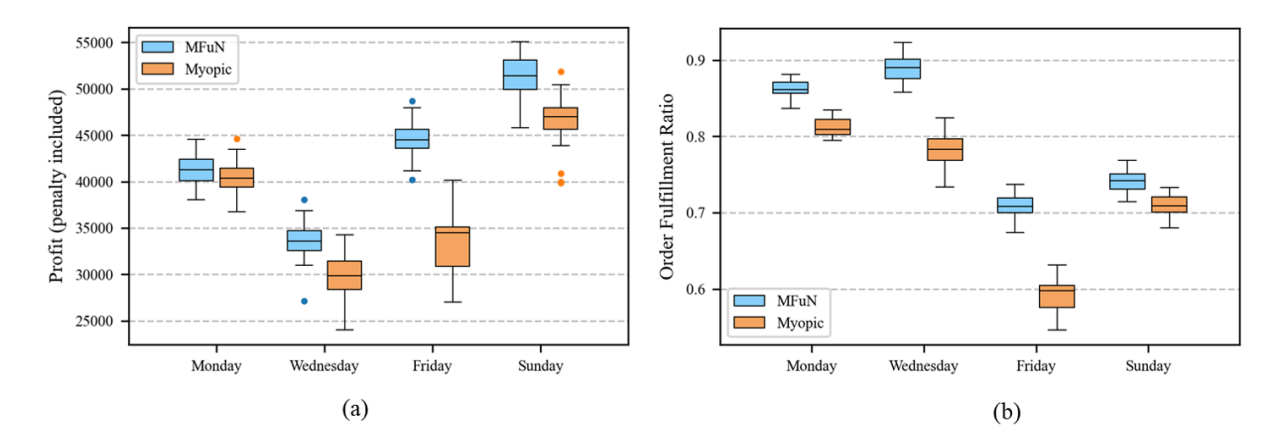


Figure 16: Performance of MFuN and Myopic in the realistic network. (a) Profit. (b) Order fulfillment ratio.

It is observed that the MFuN outperforms the myopic method under demand and supply patterns of various weekdays, attaining improvement on both average daily profit and order fulfillment ratio. The advantages of MFuN are particularly pronounced when there is a significant imbalance between demand and supply, such as during peak periods like Fridays. In this scenario, MFuN demonstrates a remarkable 27% improvement in daily profits compared to the myopic method. Under the scenario of Monday where the demand peak emerges at the beginning of a day, MFuN may not have enough time to effectively allocate resources to accommodate the sudden surge in demand. Under the Wednesday scenario, MFuN attains satisfactory order fulfillment rates when demand is relatively sparse compared to the weekend.

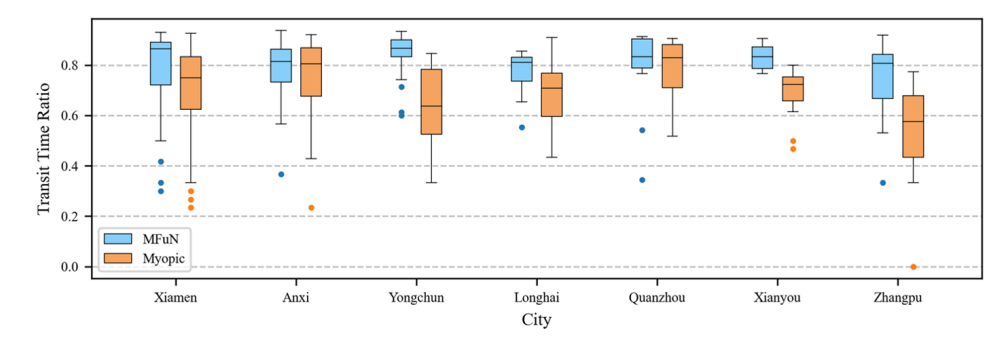


Figure 17: Average percentage of time in transit for vehicles originating from each city under the Sunday scenario.

The advantage of MFuN is reflected in the intelligent spatiotemporal allocation of vehicle resources. From a spatial perspective, MFuN dispatches all available resources in the system in a more flexible manner. Figure 17 shows the percentage of time in transit for vehicles originating

from each city under the Sunday scenario. Under the MFuN dispatching strategy, vehicles from different cities have similar transit times, indicating a balanced allocation of resources. On the other hand, under the myopic dispatching approach, vehicles originating from cities with lower demand, such as Yongchun and Zhangpu, may experience longer idle times. The proactive dispatching strategy employed by MFuN leads to improved overall utilization of vehicle resources, which aligns with the platform operator's expectations. Furthermore, the revenue distribution among drivers is also more balanced under the MFuN framework, as demonstrated in Figure 18, which indicates a more systematic task assignment facilitated by MFuN. These improvements highlight the effectiveness of agent cooperation within the multi-agent feudal networks, further enhancing the operational outcomes of the ride-pooling platform.

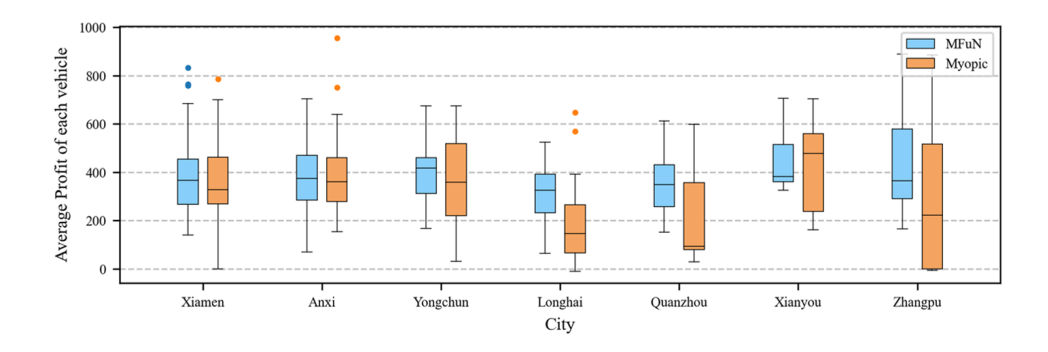


Figure 18: Average daily revenue for drivers originating from each city under the Sunday scenario.

From a temporal scheduling perspective, MFuN demonstrates its ability to identify and respond to potential fluctuations in demand and supply within specific cities (agents). This adaptability allows MFuN to make informed decisions based on anticipated dynamics. Figure 19 presents the number of departures and orders for a line with a demand peak in the afternoon. Under the MFuN framework, the demand peak of this line is recognized, prompting the dispatching of a greater number of vehicles to the originating city. As a result, vehicles can depart continuously during peak periods to fulfill orders. In contrast, the myopic method dispatches only a limited number of vehicles to the originating city during the peak periods, leading to a shortage of available vehicles and a higher rate of order loss in subsequent periods.

5.4.2 Sensitivity analysis of supply and demand level

This subsection is devoted to conducting sensitivity analyses on the performance of fleet operational strategies in relation to different supply and demand levels. The experiments on different supply levels vary on the number of vehicles applied in each line. Five supply quantity levels are set, ranging from 60% to 140% based on the fleet under the Sunday scenario in realistic operational data. The performance of both methods in terms of average daily profit and order fulfillment ratio is presented in Figure 20. A series of experiments are also conducted to explore the impact of different demand densities on the performance of the fleet operational strategies. The demand densities are varied from shrinking by 40% to amplifying by 40% based on the demand dynamics under the Sunday scenario in realistic operational data. The performance comparisons under various demand levels are shown in Figure 21.

These two series of experiments reveal consistent patterns in the performance of the two

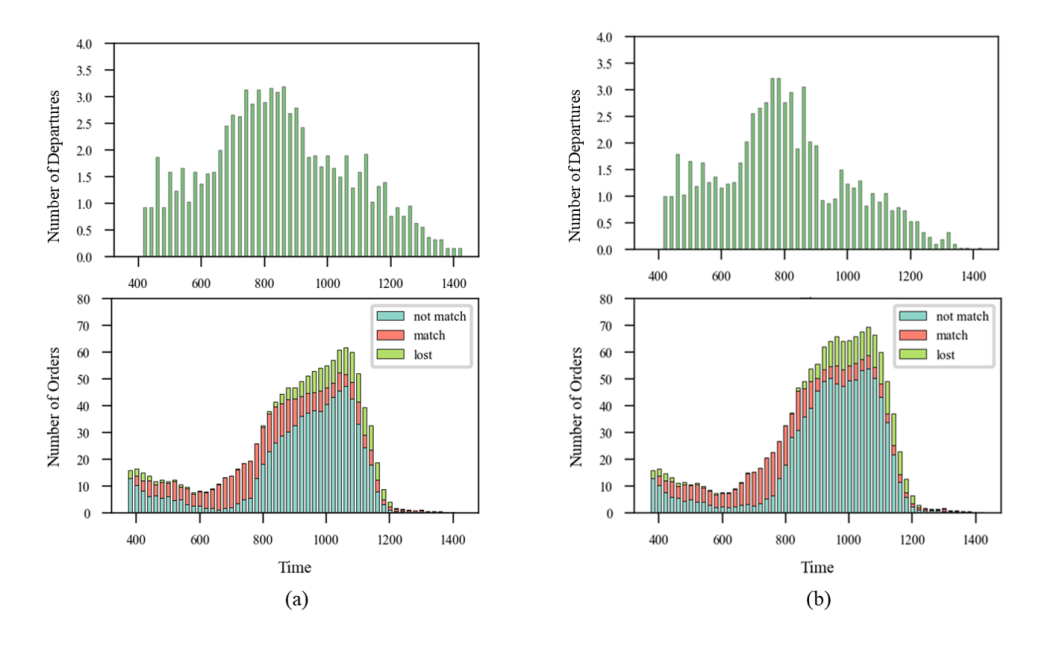


Figure 19: Number of vehicle departures and orders for a line in each period. (a) MFuN. (b) Myopic.

methods. The MFuN framework demonstrates superior performance over the myopic method when the demand levels are relatively low. This advantage arises from the ability of MFuN to intelligently allocate vehicles to high-demand lines, thereby maximizing the system's profit. Even in scenarios where the overall demand level is low or the supply level is high, there are still peak periods and lines that lack sufficient vehicles. In such cases, MFuN excels in optimizing the allocation of vehicles to high-demand lines, whereas the myopic method often results in a large number of idle vehicles in low-demand regions.

However, under conditions where the supply level is relatively low or the demand level is relatively high, vehicle resources can always be in high utilization. In these situations, the myopic method already guarantees that vehicles are utilized to their fullest capacity, leaving little room for MFuN to further improve the matching of demand and vehicle resources.

6 Conclusion

This study addresses the challenging problem of online fleet operations in on-demand intercity ride-pooling services within city clusters, characterized by a complex embedded structure. The fleet operations involve assigning idle vehicles in each city to lines and optimizing the vehicle routing for each line dynamically. The assignment of vehicles to intercity lines can be regarded as a stochastic dynamic vehicle resource allocation problem, while the online order-matching and vehicle routing process is a variant of dynamic DARP. The integrated online optimization framework of vehicle resource allocation and dynamic vehicle routing is barely touched in the literature.

To address this gap, we propose a two-level framework that combines reinforcement learning and heuristic approaches. A novel multi-agent hierarchical reinforcement learning method

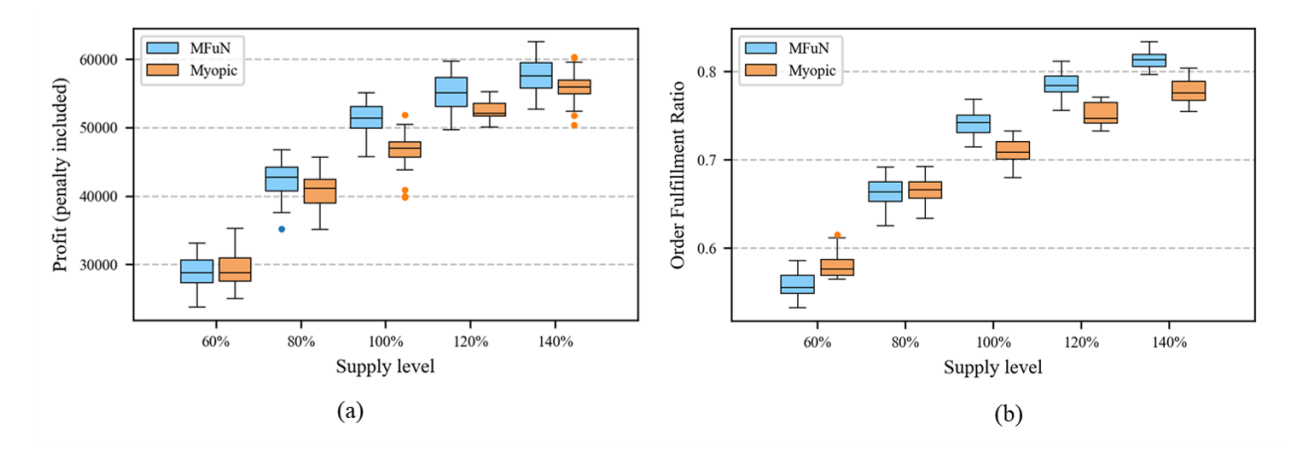


Figure 20: Performance of MFuN and Myopic under different supply levels. (a) Profit. (b) Order fulfillment ratio.

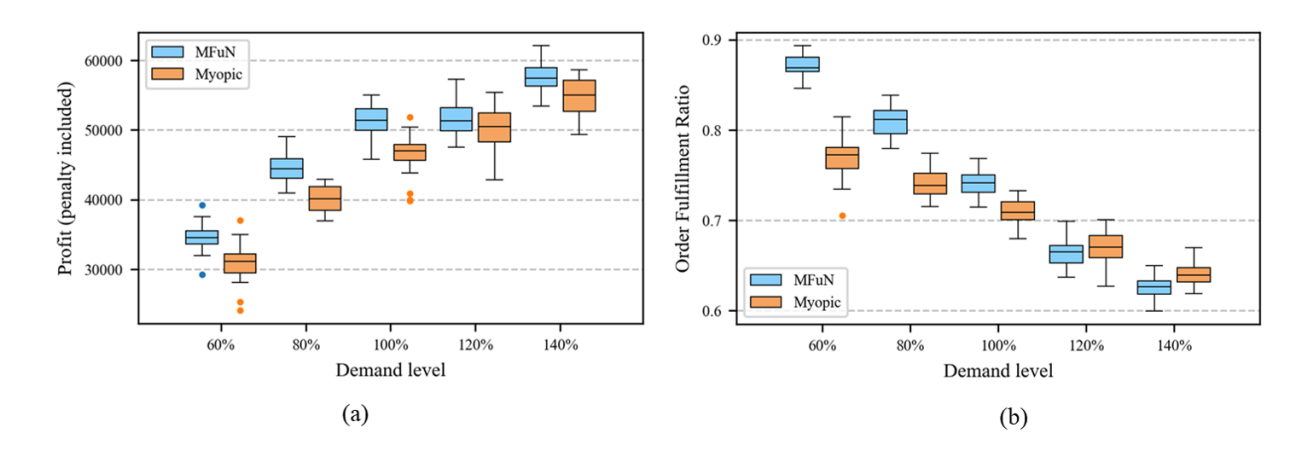


Figure 21: Performance of MFuN and Myopic under different demand levels. (a) Profit. (b) Order fulfillment ratio.

named multi-agent feudal networks is adopted in the upper level of the framework. Each worker agent corresponds to a city and collaboratively makes decisions on vehicle assignments under the guidance of a manager agent. The outputs of the worker agents, represented in a multi-discrete manner, are interpreted and mapped by a mixed-integer linear programming (MILP) formulation that considers the heterogeneity of vehicles. In the lower level of the framework, we solve the dynamic DARP using an adaptive large neighborhood search heuristic based on the assigned vehicles for each line.

We conduct extensive numerical experiments to evaluate the effectiveness of our proposed framework based on two toy networks and a realistic network in Xiamen. The experiments on the toy networks demonstrate the efficacy of our framework in temporal scheduling and spatial allocation. Furthermore, our proposed framework outperforms the myopic method across various demand and supply scenarios in the realistic network with 7 cities and 12 lines, attaining improvements in average daily profit and order fulfillment ratio. The optimization effect of MFuN is primarily observed in mitigating the spatial-temporal imbalance between supply and demand, with relatively balanced scenarios showing fewer advantages for MFuN.

In future studies, we plan to extend the scope of our research from on-demand orders to include orders with different reservation lead times. The platform can design price mechanisms to influence the stochastic demand and improve the fleet operation strategy to provide services to hybrid demand including on-demand orders and orders reserved in advance. Another area of investigation is the planning of intercity ride-pooling services within city clusters, which encompasses determining the optimal fleet size, pricing mechanisms, and operation lines. This planning can be constructed on the market equilibrium of intercity passenger transport, taking into account the competition with other intercity transit modes.

References

- Agatz, N., Erera, A., Savelsbergh, M., and Wang, X. (2012). Optimization for dynamic ridesharing: A review. *European Journal of Operational Research*, 223(2):295–303.
- Ahilan, S. and Dayan, P. (2019). Feudal multi-agent hierarchies for cooperative reinforcement learning. *arXiv preprint arXiv:1901.08492*.
- Braekers, K. and Kovacs, A. A. (2016). A multi-period dial-a-ride problem with driver consistency. *Transportation Research Part B: Methodological*, 94:355–377.
- Cordeau, J. (2006). A branch-and-cut algorithm for the dial-a-ride problem. *Operations Research*, 54(4):573–586.
- Czioska, P., Kutadinata, R., Trifunović, A., Winter, S., Sester, M., and Friedrich, B. (2019). Realworld meeting points for shared demand-responsive transportation systems. *Public Transport*, 11:341–377.
- Dayan, P. and Hinton, G. E. (1992). Feudal reinforcement learning. *Advances in neural information processing systems*, 5.
- Demir, E., Bektaş, T., and Laporte, G. (2012). An adaptive large neighborhood search heuristic for the pollution-routing problem. *European Journal of Operational Research*, 223(2):346–359.
- Fang, C. and Yu, D. (2017). Urban agglomeration: An evolving concept of an emerging phenomenon. *Landscape and urban planning*, 162:126–136.
- Fielbaum, A., Bai, X., and Alonso-Mora, J. (2021). On-demand ridesharing with optimized pick-up and drop-off walking locations. *Transportation research part C: emerging technologies*, 126:103061.
- Ganji, S., Ahangar, A., Awasthi, A., and Jamshidi Bandari, S. (2021). Psychological analysis of intercity bus passenger satisfaction using q methodology. *Transportation Research Part A: Policy and Practice*, 154:345–363.
- Ghilas, V., Demir, E., and Van Woensel, T. (2016). An adaptive large neighborhood search heuristic for the pickup and delivery problem with time windows and scheduled lines. *Computers & Operations Research*, 72:12–30.
- Godfrey, G. A. and Powell, W. B. (2002). An adaptive dynamic programming algorithm for dynamic fleet management, ii: Multiperiod travel times. *Transportation Science*, 36(1):40–54.

- Goeke, D. (2019). Granular tabu search for the pickup and delivery problem with time windows and electric vehicles. *European Journal of Operational Research*, 278(3):821–836.
- Gschwind, T. and Drexl, M. (2019). Adaptive large neighborhood search with a constant-time feasibility test for the dial-a-ride problem. *Transportation Science*, 53(2):480–491.
- Gschwind, T. and Irnich, S. (2015). Effective handling of dynamic time windows and its application to solving the dial-a-ride problem. *Transportation Science*, 49(2):335–354.
- Guo, G. and Xu, Y. (2020). A deep reinforcement learning approach to ride-sharing vehicle dispatching in autonomous mobility-on-demand systems. *IEEE Intelligent Transportation Systems Magazine*, 14(1):128–140.
- Guo, G. and Zhang, T. (2020). A residual spatio-temporal architecture for travel demand forecasting. *Transportation Research Part C: Emerging Technologies*, 115:102639.
- Guo, J., Long, J., Xu, X., Yu, M., and Yuan, K. (2022). The vehicle routing problem of intercity ride-sharing between two cities. *Transportation Research Part B: Methodological*, 158:113–139.
- Guo, X., Caros, N. S., and Zhao, J. (2021). Robust matching-integrated vehicle rebalancing in ride-hailing system with uncertain demand. *Transportation Research Part B: Methodological*, 150:161–189.
- Guo, Y., Zhang, Y., Yu, J., and Shen, X. (2020). A spatiotemporal thermo guidance based real-time online ride-hailing dispatch framework. *IEEE Access*, 8:115063–115077.
- Ho, S. C., Szeto, W. Y., Kuo, Y. H., Leung, J. M. Y., Petering, M., and Tou, T. W. H. (2018). A survey of dial-a-ride problems: Literature review and recent developments. *Transportation Research Part B-Methodological*, 111:395–421.
- Huang, D., Gu, Y., Wang, S., Liu, Z., and Zhang, W. (2020). A two-phase optimization model for the demand-responsive customized bus network design. *Transportation Research Part C: Emerging Technologies*, 111:1–21.
- Jiao, Y., Tang, X., Qin, Z. T., Li, S., Zhang, F., Zhu, H., and Ye, J. (2021). Real-world ride-hailing vehicle repositioning using deep reinforcement learning. *Transportation Research Part C: Emerging Technologies*, 130:103289.
- Jin, J., Zhou, M., Zhang, W., Li, M., Guo, Z., Qin, Z., Jiao, Y., Tang, X., Wang, C., Wang, J., et al. (2019). Coride: joint order dispatching and fleet management for multi-scale ride-hailing platforms. In *Proceedings of the 28th ACM International Conference on Information and Knowledge Management*, pages 1983–1992.
- Ke, J., Zheng, H., Yang, H., and Chen, X. M. (2017). Short-term forecasting of passenger demand under on-demand ride services: A spatio-temporal deep learning approach. *Transportation research part C: Emerging technologies*, 85:591–608.
- Kullman, N. D., Cousineau, M., Goodson, J. C., and Mendoza, J. E. (2022). Dynamic ride-hailing with electric vehicles. *Transportation Science*, 56(3):775–794.
- Lee, E., Cen, X., and Lo, H. K. (2021). Zonal-based flexible bus service under elastic stochastic demand. *Transportation Research Part E: Logistics and Transportation Review*, 152:102367.

- Lei, C., Jiang, Z. T., and Ouyang, Y. F. (2020). Path-based dynamic pricing for vehicle allocation in ridesharing systems with fully compliant drivers. *Transportation Research Part B-Methodological*, 132:60–75.
- Liu, Y. and Ouyang, Y. (2021). Mobility service design via joint optimization of transit networks and demand-responsive services. *Transportation Research Part B: Methodological*, 151:22–41.
- Liu, Y., Wu, F., Lyu, C., Li, S., Ye, J., and Qu, X. (2022). Deep dispatching: A deep reinforcement learning approach for vehicle dispatching on online ride-hailing platform. *Transportation Research Part E: Logistics and Transportation Review*, 161:102694.
- Lowe, R., Wu, Y. I., Tamar, A., Harb, J., Pieter Abbeel, O., and Mordatch, I. (2017). Multi-agent actor-critic for mixed cooperative-competitive environments. *Advances in neural information processing systems*, 30.
- Luo, Z., Liu, M., and Lim, A. (2019). A two-phase branch-and-price-and-cut for a dial-a-ride problem in patient transportation. *Transportation Science*, 53(1):113–130.
- Maciejewski, M., Bischoff, J., and Nagel, K. (2016). An assignment-based approach to efficient real-time city-scale taxi dispatching. *IEEE Intelligent Systems*, 31(1):68–77.
- Mao, C., Liu, Y., and Shen, Z.-J. M. (2020). Dispatch of autonomous vehicles for taxi services: A deep reinforcement learning approach. *Transportation Research Part C: Emerging Technologies*, 115:102626.
- Melis, L. and Sörensen, K. (2022a). The real-time on-demand bus routing problem: The cost of dynamic requests. *Computers & Operations Research*, 147:105941.
- Melis, L. and Sörensen, K. (2022b). The static on-demand bus routing problem: large neighborhood search for a dial-a-ride problem with bus station assignment. *International Transactions in Operational Research*, 29(3):1417–1453.
- MOT (2022). Statistical communiqué of the people's republic of china on the transport industry. https://xxgk.mot.gov.cn/2020/jigou/zhghs/202205/t20220524_3656659.html. Accessed May 25, 2022.
- Naccache, S., Côté, J.-F., and Coelho, L. C. (2018). The multi-pickup and delivery problem with time windows. *European Journal of Operational Research*, 269(1):353–362.
- Qin, G., Luo, Q., Yin, Y., Sun, J., and Ye, J. (2021a). Optimizing matching time intervals for ride-hailing services using reinforcement learning. *Transportation Research Part C: Emerging Technologies*, 129:103239.
- Qin, X., Yang, H., Wu, Y., and Zhu, H. (2021b). Multi-party ride-matching problem in the ride-hailing market with bundled option services. *Transportation Research Part C: Emerging Technologies*, 131:103287.
- Qin, Z., Tang, X., Jiao, Y., Zhang, F., Xu, Z., Zhu, H., and Ye, J. (2020). Ride-hailing order dispatching at didi via reinforcement learning. *INFORMS Journal on Applied Analytics*, 50(5):272–286.
- Ropke, S. and Pisinger, D. (2006). An adaptive large neighborhood search heuristic for the pickup and delivery problem with time windows. *Transportation Science*, 40(4):455–472.

- Schwieterman, J., Antolin, B., Bell, C., et al. (2021). On the brink: 2021 outlook for the intercity bus industry in the united states.
- Sun, P., Veelenturf, L. P., Hewitt, M., and Van Woensel, T. (2020a). Adaptive large neighborhood search for the time-dependent profitable pickup and delivery problem with time windows. *Transportation Research Part E-Logistics and Transportation Review*, 138.
- Sun, Q., Chien, S., Hu, D., Chen, G., and Jiang, R.-S. (2020b). Optimizing multi-terminal customized bus service with mixed fleet. *IEEE Access*, 8:156456–156469.
- Tafreshian, A., Abdolmaleki, M., Masoud, N., and Wang, H. (2021). Proactive shuttle dispatching in large-scale dynamic dial-a-ride systems. *Transportation Research Part B: Methodological*, 150:227–259.
- Tang, X., Qin, Z., Zhang, F., Wang, Z., Xu, Z., Ma, Y., Zhu, H., and Ye, J. (2019). A deep value-network based approach for multi-driver order dispatching. In *Proceedings of the 25th ACM SIGKDD international conference on knowledge discovery & data mining*, pages 1780–1790.
- Tang, X. D., Li, M., Lin, X., and He, F. (2020). Online operations of automated electric taxi fleets: An advisor-student reinforcement learning framework. *Transportation Research Part C-Emerging Technologies*, 121.
- Tong, Y., She, J., Ding, B., Chen, L., Wo, T., and Xu, K. (2016). Online minimum matching in real-time spatial data: experiments and analysis. *Proceedings of the VLDB Endowment*, 9(12):1053–1064.
- Vansteenwegen, P., Melis, L., Aktaş, D., Montenegro, B. D. G., Vieira, F. S., and Sörensen, K. (2022). A survey on demand-responsive public bus systems. *Transportation Research Part C: Emerging Technologies*, 137:103573.
- Vezhnevets, A. S., Osindero, S., Schaul, T., Heess, N., Jaderberg, M., Silver, D., and Kavukcuoglu, K. (2017). Feudal networks for hierarchical reinforcement learning. In *International Conference on Machine Learning*, pages 3540–3549. PMLR.
- Wang, H. and Yang, H. (2019). Ridesourcing systems: A framework and review. *Transportation Research Part B: Methodological*, 129:122–155.
- Wu, Y., Poon, M., Yuan, Z., and Xiao, Q. (2022). Time-dependent customized bus routing problem of large transport terminals considering the impact of late passengers. *Transportation Research Part C: Emerging Technologies*, 143:103859.
- Xu, Z., Li, Z., Guan, Q., Zhang, D., Li, Q., Nan, J., Liu, C., Bian, W., and Ye, J. (2018a). Large-scale order dispatch in on-demand ride-hailing platforms: A learning and planning approach. In *Proceedings of the 24th ACM SIGKDD International Conference on Knowledge Discovery & Data Mining*, pages 905–913.
- Xu, Z., Li, Z. X., Guan, Q. W., Zhang, D. S., Li, Q., Nan, J. X., Liu, C. Y., Bian, W., Ye, J. P., and Acm (2018b). Large-scale order dispatch in on-demand ride-hailing platforms: A learning and planning approach. In 24th ACM SIGKDD Conference on Knowledge Discovery and Data Mining (KDD), pages 905–913.
- Yang, H., Qin, X., Ke, J., and Ye, J. (2020). Optimizing matching time interval and matching radius in on-demand ride-sourcing markets. *Transportation Research Part B: Methodological*, 131:84–105.

Yu, X. and Shen, S. (2019). An integrated decomposition and approximate dynamic programming approach for on-demand ride pooling. *IEEE Transactions on Intelligent Transportation Systems*, 21(9):3811–3820.

Appendix A: Notations

Table A.1: Notations for the fleet dispatching and vehicle routing model

| Notations | Explanation |
|---|--|
| Sets | |
| \mathcal{U} | the set of cities |
| $\mathcal L$ | the set of intercity lines |
| ${\mathcal T}$ | the set of dispatching horizons |
| \mathcal{K}_u^t | the set of available vehicles for assignment at horizon t at city u |
| $\hat{\mathcal{K}}_{u}^{t}$ | the set of vehicles that newly enter the system at horizon t at city u |
| $	ilde{\mathcal{K}}_{u}^{	ilde{t}}$ | the set of vehicles that exit the system at horizon t at city u |
| $\check{\mathcal{K}}_{u}^{\widetilde{t}}$ | the set of arrived vehicles at horizon t at city u |
| $ar{\mathcal{K}}_{u}^{	ilde{t}}$ | the set of reserved vehicles at horizon t at city u |
| \mathcal{K}_{u}^{t} $\hat{\mathcal{K}}_{u}^{t}$ $\tilde{\mathcal{K}}_{u}^{t}$ $\tilde{\mathcal{K}}_{u}^{t}$ $\tilde{\mathcal{K}}_{u}^{t}$ $\tilde{\mathcal{K}}_{u}^{t}$ $\tilde{\mathcal{K}}_{u}^{t}$ | the set of vehicles that exit the system due to reaching limited work |
| | duration at horizon t at city u |
| \mathcal{N}_{uv}^t | the set of vehicles dispatched from city u to city v at horizon t |
| \mathcal{K}_{uv}^{uv} | the set of vehicles en route of line (u, v) |
| \mathcal{O}_{uv} | the set of orders in the matching pool and in service for line (u, v) |
| \mathcal{O}_{uv}^1 | the set of orders for line (u, v) that passengers have been picked |
| \mathcal{O}_{uv}^{2} | the set of orders for line (u, v) that have been matched but not picked |
| \mathcal{O}_{uv}^3 | the set of orders in matching pool of line (u, v) |
| \mathcal{V}_k | the set of vehicle locations at the beginning of a matching interval |
| \mathcal{K}_{uv} \mathcal{O}_{uv} \mathcal{O}^1_{uv} \mathcal{O}^2_{uv} \mathcal{O}^3_{uv} \mathcal{V}_k \mathcal{V}_f | the set of destination nodes of all orders |
| $\mathcal{V}_s^{'}$ | the set of origin nodes of the unserved orders |
| Parameters | |
| $ar{W}$ | maximum daily work time for a driver |
| R^{uv} | trip fare of line (u, v) |
| С | traveling cost per unit of distance |
| p_e | the penalty rate for losing one passenger |
| v_k | location of vehicle <i>k</i> at the beginning of a matching interval |
| n_p | number of passengers of order <i>p</i> |
| s_p | origin node of order <i>p</i> |
| $f_{v}^{'}$ | destination node of order <i>p</i> |
| $egin{aligned} f_p \ [\check{L}_p, \check{U}_p] \ [\hat{L}_p, \hat{U}_p] \end{aligned}$ | time window of origin node of order <i>p</i> |
| $[\hat{L}_n, \hat{U}_n]$ | time window of destination node of order <i>p</i> |
| k_p | matched vehicle of order $p \in O_{uv}^1 \cup O_{uv}^2$ |
| É | the location of the depot in the destination city |
| D_{ij} | the distance of arc (i, j) in the graph for routing |
| W | the capacity of the vehicle |
| Variables | |
| s_k^t | the number of passengers that vehicle k picked in the trip begins at |
| κ | horizon t |
| ϵ_{uz}^t | the number of lost passengers in line (u, v) at horizon t |
| $egin{aligned} \epsilon_{uv}^t \ \delta_k^t \ \epsilon_{uv}^t \end{aligned}$ | the total distance of the trip of vehicle k begins at horizon t |
| c K | the number of lost passengers in line (u, v) at horizon t |

| Notations | Explanation | |
|---------------------|--|--|
| Decision variables | | |
| x_{ij}^{pk} | binary variable indicating whether vehicle k passes arc (i, j) with pas- | |
| • | sengers of order p | |
| $y_{ij}^k \ d_{pk}$ | binary variable indicating whether vehicle k passes arc (i, j) | |
| d_{pk} | binary variable indicating whether vehicle k serves order p | |
| u_{kj} | the time for vehicle k to arrive at node j . The constraints can be for- | |
| | mulated as follows | |